

## General Disclaimer

### One or more of the Following Statements may affect this Document

- This document has been reproduced from the best copy furnished by the organizational source. It is being released in the interest of making available as much information as possible.
- This document may contain data, which exceeds the sheet parameters. It was furnished in this condition by the organizational source and is the best copy available.
- This document may contain tone-on-tone or color graphs, charts and/or pictures, which have been reproduced in black and white.
- This document is paginated as submitted by the original source.
- Portions of this document are not fully legible due to the historical nature of some of the material. However, it is the best reproduction available from the original submission.



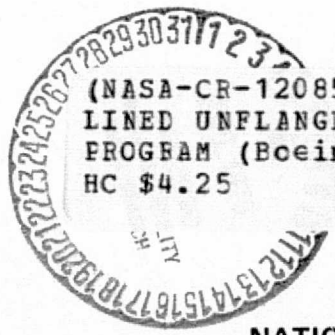
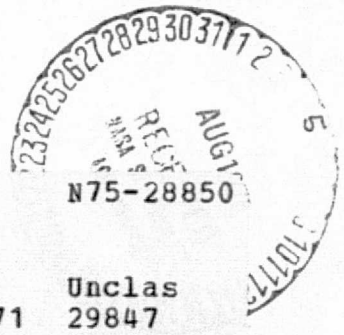
# ACOUSTIC RADIATION FROM LINED, UNFLANGED DUCTS — DIRECTIVITY INDEX PROGRAM

BY  
R. J. BECKEMEYER AND D. T. SAWDY

DECEMBER 12, 1971

THE **BOEING** COMPANY  
WICHITA DIVISION - WICHITA, KANSAS. 67210

(NASA-CR-120850) ACOUSTIC RADIATION FROM  
LINED UNFLANGED DUCTS: DIRECTIVITY INDEX  
PROGRAM (Boeing Co., Wichita, Kans.) 67 p  
HC \$4.25 CSCL 20A



Unclas  
29847  
G3/71

PREPARED FOR  
NATIONAL AERONAUTICS AND SPACE ADMINISTRATION

NASA-LEWIS RESEARCH CENTER  
CONTRACT NAS 3-14321  
H. BLOOMER, PROJECT MANAGER

TOPICAL REPORT

ACOUSTIC RADIATION FROM LINED, UNFLANGED DUCTS —  
DIRECTIVITY INDEX PROGRAM

by  
R. J. Beckemeyer and D. T. Sawdy

THE BOEING COMPANY  
3801 SOUTH OLIVER  
WICHITA, KANSAS 67210

Prepared For  
NATIONAL AERONAUTICS AND SPACE ADMINISTRATION  
December 12, 1971

CONTRACT NASA 3-14321

NASA-LEWIS RESEARCH CENTER  
CLEVELAND, OHIO  
H. BLOOMER, PROJECT MANAGER  
V/STOL AND NOISE DIVISION

## FOREWORD

The work described herein was done by The Boeing Company, Wichita Division, under NASA contract NAS 3-14321 with Mr. H. Bloomer, V/STOL and Noise Division, NASA - Lewis Research Center, as Project Manager.

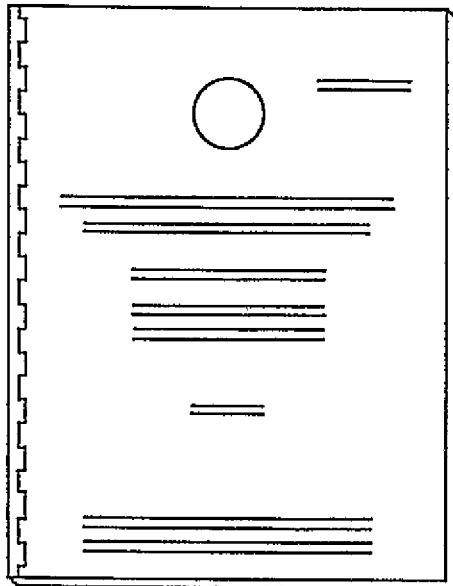
## ABSTRACT

An acoustic radiation analysis has been developed to predict the far-field characteristics of fan noise radiated from an acoustically lined unflanged duct. This analysis is comprised of three modular digital computer programs which together provide a capability of accounting for the impedance mismatch at the duct exit plane. This report discusses the Directivity Index Program whose relationship with the other two modular reports of the analysis is illustrated on the following page.

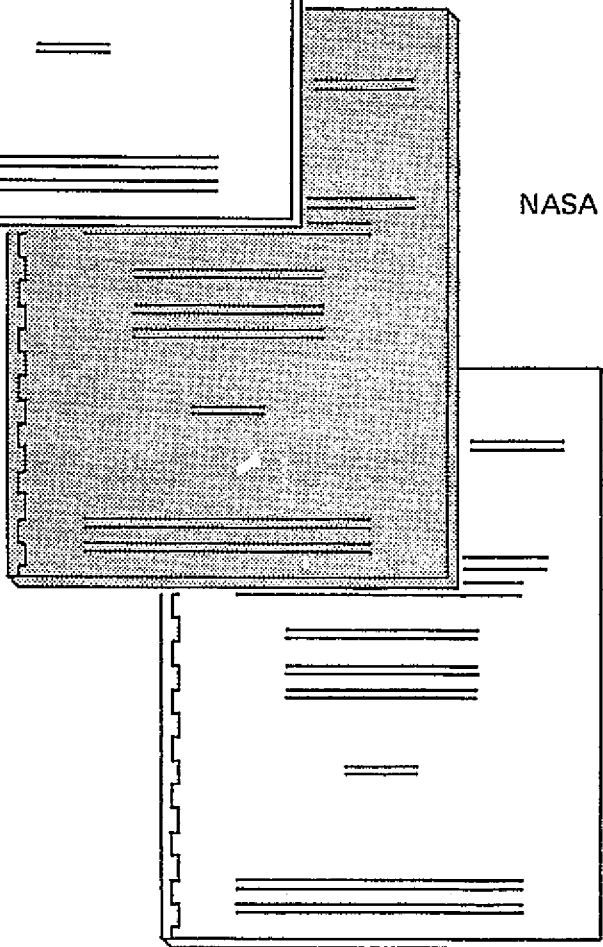
Admissible duct configurations include circular or annular, with or without an extended centerbody. This variation in duct configurations provides a capability of modeling inlet and fan duct noise radiation.

DEVELOPMENT OF ACOUSTIC RADIATION ANALYSIS  
OF TURBOFAN NOISE FROM LINED, UNFLANGED DUCTS

OVERALL REPORT ORGANIZATION



NASA CR 120849 – ACOUSTIC SOURCE DISTRIBUTION  
PROGRAM



NASA CR 120850 – DIRECTIVITY INDEX  
PROGRAM

NASA CR 120851 –  
DUCT TERMINATION  
IMPEDANCE PROGRAM

## TABLE OF CONTENTS

	PAGE
NOMENCLATURE . . . . .	vi
INDEX OF FIGURES . . . . .	vii
1.0 INTRODUCTION . . . . .	1
1.1 Background . . . . .	1
1.2 Technical Approach . . . . .	1
2.0 MATHEMATICAL DEVELOPMENT . . . . .	3
3.0 METHOD OF SOLUTION . . . . .	7
4.0 RESULTS . . . . .	11
4.1 Application . . . . .	11
4.2 Limitations . . . . .	11
5.0 CONCLUSIONS AND RECOMMENDATIONS . . . . .	13
6.0 REFERENCES . . . . .	15
7.0 FIGURES . . . . .	17
APPENDIX 1 – PROGRAM DESCRIPTION . . . . .	23
Nomenclature	
Input	
Program Flow	
Output	
APPENDIX 2 – PROGRAM FLOW CHART . . . . .	29
APPENDIX 3 – MAIN PROGRAM LISTING . . . . .	37
APPENDIX 4 – GAUSS SUBROUTINE LISTING . . . . .	45
APPENDIX 5 – BESJY SUBROUTINE LISTING . . . . .	51
APPENDIX 6 – EXAMPLE PROBLEM . . . . .	53
Listing of Input Data	
Output for Example Problem	

## NOMENCLATURE

### Analytical Variables

$a$	Centerbody Radius
$b$	Outer Duct Radius
$c$	Sound Speed in Air
$G(\psi)$	Directivity Function
$J_m(Z)$	Bessel Function of 1st Kind and Order $m$
$k$	Wavenumber, $k = \omega/c$
$m$	Angular Mode No.
$p$	Far-field Pressure
$P$	Far-field Point
$r$	Radial Coordinate
$r_j$	Radial Coordinate Integration Variable
$R$	Distance between Points
$R_j$	Distance between Point on Duct and Field Point
$s$	Separation distance
$t$	Time
$u$	Radial Velocity Component
$v$	Axial Velocity Component
$V$	Velocity Distribution on Exit Face
$z$	Axial Coordinate
$\Delta r$	Annular ring box length
$\Delta z$	Axial box length
$\theta$	Angular Coordinate
$\theta_j$	Angular Coordinate Integration Variable
$\rho$	Air Density
$\phi$	Velocity Potential
$\phi_j$	Source Strength Distribution
$\psi$	Polar Angle
$\omega$	Frequency, Radians/Second



## INDEX OF FIGURES

<u>FIGURE</u>		<u>PAGE</u>
1	Admissible Duct Configurations . . . . .	19
2	Geometry . . . . .	20
3	Box Method Integration and Control Blocks . . . . .	21
4	Example Problem Normalized Directivity Pattern . . . . .	22

## 1.0 INTRODUCTION

### 1.1 Background

This report discusses the Directivity Index Program that provides the radiation portion of the package of modular computer programs which together form a first generation capability for the analytical prediction of far field noise being radiated from an unflanged inlet or exhaust duct.

The development of this program had its origin in the need for a method to determine the directional distribution of acoustic energy in the far field which is radiated into free space from the fluctuating pressure field appearing at the open face of an unflanged duct.

This digital computer program utilizes the output from the Acoustic Source Distribution Program, Reference 1, to generate the far-field radiation patterns for a duct with no open-end correction. The impedance mismatch at the duct face can be accounted for by the Duct Termination Impedance Program, Reference 2, to determine the correct pressure distribution on the open duct face.

### 1.2 Technical Approach

This technical development addresses the far-field radiation pattern that is generated from fan or compressor noise exiting from an inlet or exhaust duct. Unflanged ducts with both annular and circular cross-sections can be analyzed by the program. The option of extending the centerbody beyond the duct face permits the program to analyze the three duct configurations shown in Figure 1. Any combination of these configurations may be superimposed to model a specific engine geometry. For example, by representing an engine exhaust duct with Configuration B and superimposing it upon Configuration A which represents the inlet, the far-field radiation patterns are calculated for the inlet and exhaust separately and then combined.

The approach presented is an extension of the case of sound radiating from a duct enclosed by an infinite baffle to the unflanged case which accounts for the diffraction of sound around the outside lip of the duct. The phased contributions of the outer and extended inner duct surfaces to the total far-field pressure must be determined and then combined with the radiation of acoustic energy from the duct face.

The far-field radiation characteristics of the duct configuration are determined from the spatial distributions of acoustic sources over the duct walls and exit plane. The source distribution which satisfies the imposed boundary conditions is determined by the Acoustic Source Distribution Program, Reference 1. These boundary conditions require that the acoustic perturbation velocity normal to the outer duct walls must vanish. In addition, the normal velocity distribution over the duct exit plane must equal the velocity distribution associated with either a single mode or a combination of modes of discrete frequency.

Given the source distribution over the duct, the far-field directivity is found by numerical integration of the Helmholtz integrals for the velocity potential (under the far-field assumptions) over the duct walls and exit plane. Far-field radiation patterns can be determined separately for the inlet and exhaust ducts and then combined.

Several assumptions have been made in this development. These concern the transport characteristics of the model and the decomposition of the acoustic sound energy into the acoustic modes present in the duct. The acoustic sound is assumed to be radiated through an inviscid perfect gas which has no mean flow. This simplification will not significantly affect the results for noise propagation through a locally subsonic flow field of an inlet. Radiation of sound through an exhaust or jet flow, a case where the refraction of sound due to the velocity gradients is important, will not be represented properly by this model.

The velocity distribution is assumed to have a  $\text{Cos}(m\theta)$  type of angular dependence. This simplification is justified by the angular characteristic functions determined from the solution of the governing wave equation for sound propagation through annular ducts. This assumption does not affect the ability to couple different modes in the far-field program, but does not restrict the Duct Termination Impedance Program, Reference 2, to the extent that for a velocity distribution whose angular dependence is specified by a combination of different  $m$  angular modes, a separate analysis must be made for each set of angular modes.

## 2.0 MATHEMATICAL DEVELOPMENT

The far-field radiation characteristics of an unflanged duct configuration are formulated in terms of the acoustic velocity potential. This formulation provides a mathematical model with a straight forward method of satisfying the velocity boundary conditions on the duct walls and exit plane. Refraction of sound from the duct interior face to the far-field is inherently accounted for in the phase relationship of the potential function.

Since the velocity potential is governed by a linear set of equations, superposition may be used to determine the far-field potential  $\phi$ . The far-field potential for the math model shown in Figure 2, is determined by the superposition of three potentials,  $\phi_0$ ,  $\phi_1$ ,  $\phi_2$ , which represent the contribution of the duct face, outer duct wall and extended inner duct wall, respectively. This technique is expressed mathematically by

$$\phi(r, \theta, z, t) = \phi_0 + \phi_1 + \phi_2 \quad (1)$$

The component velocity potentials are determined by a spatial distribution of monopole acoustic sources on each reflecting surface. For example, the velocity potential due to a distribution of harmonically vibrating sources on the face of the duct is

$$\phi_0 = e^{-i\omega t} \int_0^b \int_0^{2\pi} \frac{\Phi_0(r_0) e^{i\omega R_0/c}}{R_0} \cos(m\theta_0) r_0 d\theta_0 dr_0 \quad (2)$$

The form of this integral equation is derived from the following assumptions:

- Acoustic velocity at the point P may be determined from a monopole acoustic source,  $e^{-i(\omega t - kR_0)} / R_0$  which represents an outward propagating wave and is a solution of wave equation in spherical coordinates.
- The angular dependence of the potential may be described in terms of the characteristic function  $\text{Cos}(m\theta)$  for a given angular mode number m.
- The radial distribution of sources is given by the spatial distribution function  $\Phi_0(r)$  which is determined by the Acoustic Source Distribution Program, Reference 1.

Similarly, the velocity potential terms for the outer and inner duct wall surfaces, respectively are

$$\phi_1 = e^{-i\omega t} \int_{-\infty}^0 \int_0^{2\pi} \frac{\Phi_1(z_1) e^{i\omega R_1/c}}{R_1} \cos(m\theta_1) d\theta_1 dz_1 \quad (3)$$

$$\phi_2 = e^{-i\omega t} \int_0^\infty \int_0^{2\pi} \frac{\Phi_2(z_2) e^{i\omega R_2/c}}{R_2} \cos(m\theta_2) d\theta_2 \alpha dz_2 \quad (4)$$

The classical method of evaluating these integrals is to utilize the far-field approximations, that is, the distance between the source and the far-field point is much greater than the argument of the source strength.

$$s \gg r_0$$

The separation distance  $R_0$  in spherical coordinates

$$R_0^2 = s^2 - 2sr_0 \sin \psi \cos(\theta - \theta_0)$$

may be approximated by

$$R_0 \approx s - r_0 \sin \psi \cos(\theta - \theta_0)$$

In the exponential term and

$$\frac{1}{R_0} \approx \frac{1}{s}$$

in the reciprocal term.

The separation distances for the outer and extended inner duct surfaces are approximated by expanding the radical expression for  $R_1$  and  $R_2$  with the truncated binominal expansion.

$$R_1 \approx \sqrt{s^2 - 2sz_1 \cos \psi + z_1^2} - b \sin \psi \cos(\theta - \theta_1)$$

$$\frac{1}{R_1} \approx \frac{1}{\sqrt{s^2 - 2sz_1 \cos \psi + z_1^2}} = \frac{1}{u_1}$$

$$R_2 \approx \sqrt{s^2 - 2sz_2 \cos \psi + z_2^2} - a \sin \psi \cos(\theta - \theta_2)$$

$$\frac{1}{R_2} \approx \frac{1}{\sqrt{s^2 - 2sz_2 \cos \psi + z_2^2}} = \frac{1}{u_2}$$

Utilizing the far-field approximations in the integral Equations (2) through (4) the far-field potential of Equation (1) becomes

$$\begin{aligned}
 \phi = & \frac{e^{i\omega s/c}}{s} \int_a^b \phi_0(r_0) \int_0^{2\pi} e^{-i\frac{\omega}{c} r_0 \sin \psi \cos(\theta - \theta_0)} \cos(m\theta_0) r_0 d\theta_0 dr_0 \\
 & + \int_{-\infty}^0 \frac{\phi_1(z_1) e^{i\frac{\omega}{c} u_1}}{u_1} dz_1 \int_0^{2\pi} e^{-i\frac{\omega}{c} b \sin \psi \cos(\theta - \theta_1)} \cos(m\theta_1) b d\theta_1 \\
 & + \int_0^{\infty} \frac{\phi_2(z_2) e^{i\frac{\omega}{c} u_2}}{u_2} dz_2 \int_0^{2\pi} e^{-i\frac{\omega}{c} a \sin \psi \cos(\theta - \theta_1)} \cos(m\theta_2) a d\theta_2
 \end{aligned} \tag{5}$$

A transformation of the trigonometric functions and the definition of the Bessel function of the first kind:

$$J_m(z) = \frac{i^{-m}}{\pi} \int_{-\pi}^{\pi} e^{iz \cos \theta} \cos(m\theta) d\theta \tag{6}$$

permits the  $\theta$  integration to be made in closed form.

Utilizing Equation (6) and collecting terms, the potential function in Equation (1) can be written in terms of the directivity functions.

$$\phi = 2\pi (-i)^m \cos m\theta \frac{e^{i\omega s/c}}{s} \left[ G_0(\psi) + G_1(\psi) + G_2(\psi) \right] \tag{7}$$

The directivity functions which indicate the contribution of the duct face, outer and extended inner duct walls to the directional distribution of energy in the far-field are defined as

$$G_0(\psi) = \int_a^b \phi_0(r_0) J_m\left(-\frac{\omega}{c} r_0 \sin \psi\right) r_0 dr_0 \tag{8}$$

$$G_1(\psi) = sb J_m\left(\frac{\omega}{c} b \sin \psi\right) \int_{-\infty}^0 \frac{e^{i\frac{\omega}{c}(u_1 s)}}{u_1} \phi_1(z_1) dz_1 \tag{9}$$

$$G_2(\psi) = sa J_m\left(\frac{\omega}{c} a \sin \psi\right) \int_0^\infty \frac{e^{i\frac{\omega}{c}(u_2 - s)}}{u_2} \phi_2(z_2) dz_2 \quad (10)$$

The far-field acoustic pressure is determined from the velocity potential and the density of air, denoted by  $\rho$ .

$$p = \rho \frac{\partial \phi}{\partial t}$$

For harmonic motion, the velocity potential expressed by Equation (7) results in the following relation:

$$p = 2\pi(-i)^{m+1} \rho \omega \cos m\theta \frac{e^{i\frac{\omega}{c}s}}{s} \left[ G_0(\psi) + G_1(\psi) + G_2(\psi) \right]$$

### 3.0 METHOD OF SOLUTION

The constraint that this program must be compatible with the Acoustic Source Distribution Program of Reference 1, required that the "Box Method" technique be used to solve Equations (8) through (10). This mathematical technique assumes that the variation of the source distribution over a small portion or box of the reflecting surface is constant, an assumption which allows the integrations to be evaluated by a summation. To facilitate the numerical solution of these equations, the duct exterior face is divided into a sequence of M annular rings, and the duct walls into N and N2 cylindrical segments as shown in Figure 3.

Application of the box method to  $G_o(\psi)$ , the duct face contribution to the far-field velocity potential, enables the integral equation to be written as

$$G_o(\psi) = \sum_{j=1}^M \int_{\Delta r_j} \phi_o(r_j) J_m \left( \frac{\omega}{c} r_j \sin \psi \right) r_j dr_j \quad (11)$$

where the locations at the control points are

$$r_j = r_{j-1} + \frac{\Delta r_j + \Delta r_{j-1}}{2} \quad \text{for } j \geq 2$$

and

$$r_j = \frac{\Delta r_j}{2} + a \quad \text{for } j=1$$

For the duct wall components, the equations become

$$G_1(\psi) = sb J_m \left( \frac{\omega}{c} b \sin \psi \right) \sum_{j=1}^N \phi_1(z_{1,j}) \int_{\Delta z_{1,j}} \frac{e^{i \frac{\omega}{c} (u_1 - s)}}{u_1} dz_1 \quad (12)$$

where the locations of the control points are

$$z_{1,j} = z_{1,j-1} + \frac{\Delta z_{1,j} + \Delta z_{1,j-1}}{2}$$



$$G_2(\psi) = sa J_m\left(\frac{\omega}{c} a \sin \psi\right) \sum_{j=1}^{N2} \phi_2(z_{2,j}) \int_{\Delta z_{2,j}} \frac{e^{i\frac{\omega}{c}(u_2-s)}}{u_2} dz_2 \quad (13)$$

where the locations at the control points are

$$z_{2,j} = z_{2,j-1} + \frac{\Delta z_{2,j} + \Delta z_{2,j-1}}{2}$$

Equations (11) through (13) are integrated numerically. The numerical technique used is an even order Gaussian quadrature scheme. The integration for each annular segment is performed by an iterative method. An initial even order quadrature is chosen (usually 2nd or 4th order) and the integral evaluated. The order is increased by 2 and the integration repeated.

The two values of the integral are compared. If they agree to within a specified error, the next segment is integrated. If agreement is not obtained, the order is again increased and the procedure repeated up to a specified maximum order. At this point the last calculated value of the integral is used and the integration procedure passes to the next segment.

The quadrature method used is the Gaussian formula for arbitrary intervals.

$$\int_a^b f(x) dx = \frac{b-a}{2} \sum_{j=1}^{NG} f(x_j) w_j \quad (14)$$

This relation states that the integral may be approximated by a summation of NG (the order of the quadrature) evaluations of the function at a prescribed abscissa,  $x_j$ , which are multiplied by the associated weight,  $w_j$ . The abscissae and weights of the Gaussian quadrature may be found in Reference 3. The referenced abscissae have the normalized range  $-1 < y < 1$  and are related to the arbitrary interval abscissae by

$$x_j = \frac{(b+a)}{2} + \frac{(b-a)}{2} y_j$$

The numerical equations for the evaluation of the directivity functions are

$$G_0(\psi) = \sum_{j=1}^M \phi_0(r_j) \sum_{k=1}^{NG} J_m\left(\frac{\omega}{c} r_{jk} \sin \psi\right) r_{jk} w_k \Delta r_j \quad (15)$$

The quadrature points on the duct face are

$$r_{jk} = r_j + \frac{\Delta r_j x_k}{2}$$

$$G_1(\psi) = sb J_m\left(\frac{\omega}{c} b \sin \psi\right) \sum_{j=1}^N \phi_1(z_{1,j}) \sum_{k=1}^{NG} \frac{e^{i\frac{\omega}{c}(u_{1,j}-s)}}{u_{1,j}} w_k \Delta z_{1,j} \quad (16)$$

The quadrature points on the outer duct wall are

$$z_{1,jk} = z_{1,j} - \frac{\Delta z_{1,j} x_k}{2}$$

$$G_2(\psi) = sa J_m\left(\frac{\omega}{c} a \sin \psi\right) \sum_{j=1}^{N2} \phi_2(z_{2,j}) \sum_{k=1}^{NG} \frac{e^{i\frac{\omega}{c}(u_{2,j}-s)}}{u_{2,j}} w_k \Delta z_{2,j} \quad (17)$$

The quadrature points on the extended centerbody duct wall are

$$z_{2,jk} = z_{2,j} + \frac{\Delta z_{2,j} x_k}{2}$$

## 4.0 RESULTS

### 4.1 Application

The numerical techniques developed in Section 3 are applied to the mathematical representation of the radiation problem developed in the Acoustic Source Distribution Program, Reference 1. Duct segmentation parameters and corresponding source distributions are input to this program to determine the far-field radiation characteristics of the duct configuration. Far-field directivity patterns are determined for each mode and then combined to yield the total noise signature. In the event both an inlet and fan duct are to be modeled, their respective far-field directivity patterns can be calculated and then combined to yield the total noise signature of the nacelle.

An example duct radiation problem is presented to illustrate the output of this program. A source distribution which was generated by Reference 1 for a plane wave velocity distribution on the face of a circular duct (example problem 1) was input to this program. The resulting normalized far-field radiation pattern shown on a polar plot in Figure 4, for a circular duct with  $kb = 1.0$ , is compared with results obtained by a numerical calculation based on the closed form solution given by Reference 4. Comparison of the two results indicates that for this case the analysis does not predict the sideline portion of the directivity pattern very well.

### 4.2 Limitations

There are several limitations to this analytical program. First the effects of a mean flow within the duct on the radiation of sound has been neglected. Although application of this analysis to a nacelle radiation problem does not yield an exact model, it is anticipated that this simplification will not significantly affect results for noise propagation through a locally subsonic flow field of an inlet. However, radiation through an exhaust or jet flow will not be represented properly by the present analysis.

The second limitation to the program is restriction of the specified velocity distribution on the face of the duct to a  $\cos(m\theta)$  type of angular dependence. This assumption does not affect the capability of the program to combine different  $m$  angular modes in the far-field by superposition of the source distributions. It does, however, restrict the Duct Termination Impedance Program, Reference 2, to the extent that for a velocity distribution whose angular dependence is specified by a combination of different  $m$  angular modes a separate analysis must be made for each set of angular modes.

**PRECEDING PAGE BLANK NOT FILMED**

## 5.0 CONCLUSIONS AND RECOMENDATIONS

An acoustic radiation analysis has been developed that predicts the angular distribution of acoustic energy in the far-field that is radiated from an unflanged duct. In spite of its many advantages, this acoustic radiation analysis is limited in its range of application. For this reason, this analysis has been relegated to the role of a first generation analysis in a commitment to develop an analytical package which will predict radiation characteristics of a turbofan jet engine. As discussed in Reference 1, the present version of the analysis reaches optimum efficiency when it is applied to low frequency noise radiating from an infinite duct. This and the other limitation due to a  $\text{Cos}(m\theta)$  type of dependence of the velocity distribution are an inherent property of the "box method" numerical technique.

A second generation version of the program could avoid these limitations by utilizing a collocation technique of evaluating the integrals of Equations (8) through (10). The primary feature of this technique is that a selected analytical expression is used to represent the source distribution. The time saving feature of the collocation technique is that it requires fewer evaluations of the integrals. The collocation procedure would enable the analysis to handle any combination of angular modes, a result which would remove the angular modal coupling limitation for the Impedance Program, Reference 2, and eliminate the need for a large number of angular boxes.

In addition to the collocation procedure, a second generation version of the analysis should contain a method of accounting for a mean flow within the duct. This method should account for the effects of velocity gradients on the distortion of the radiation field by the jet.

**PRECEDING PAGE BLANK NOT FILMED**

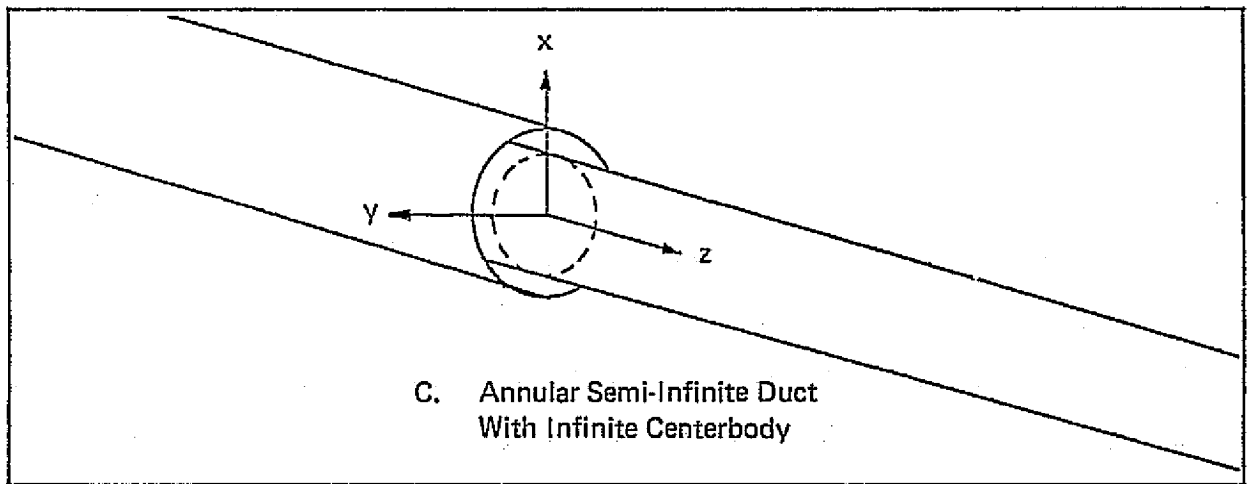
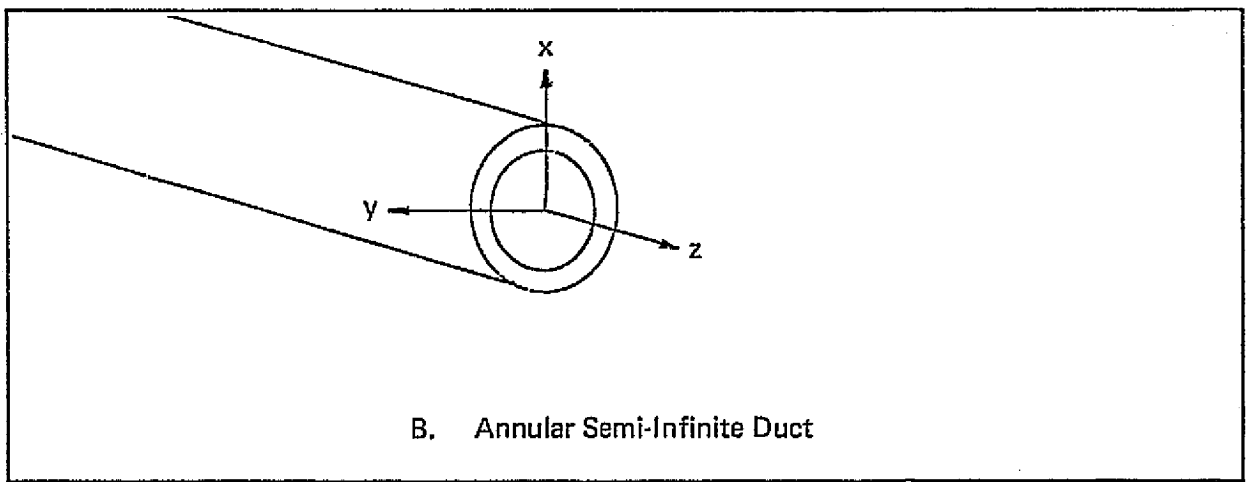
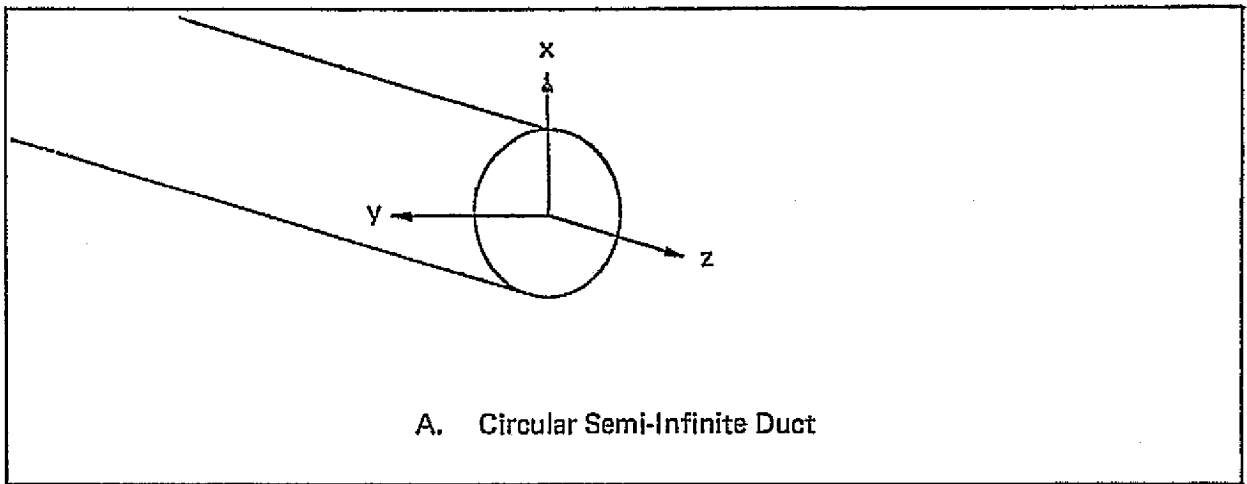
## 6.0 REFERENCES

1. Beckemeyer, R. and Sawdy, D., "Acoustic Radiation from Lined Unflanged Ducts - Acoustic Source Distribution Program," NASA CR 120849, December 1971.
2. Beckemeyer, R. and Sawdy, D., "Acoustic Radiation from Lined Unflanged Ducts - - Duct Termination Impedance Program," NASA CR 120851, December 1971.
3. Abramowitz and Stegun, "Handbook for Mathematical Functions," Dover Publications, 1965.
4. Lansing, D. L., Drischler, J. A., and Pusey, C. G., "Radiation of Sound from an Unflanged Duct with Flow," Paper presented at the 79th Meeting of the Acoustical Society of America, Atlantic City, N. J., April 21-24, 1970.

PRECEDING PAGE BLANK NOT FILMED

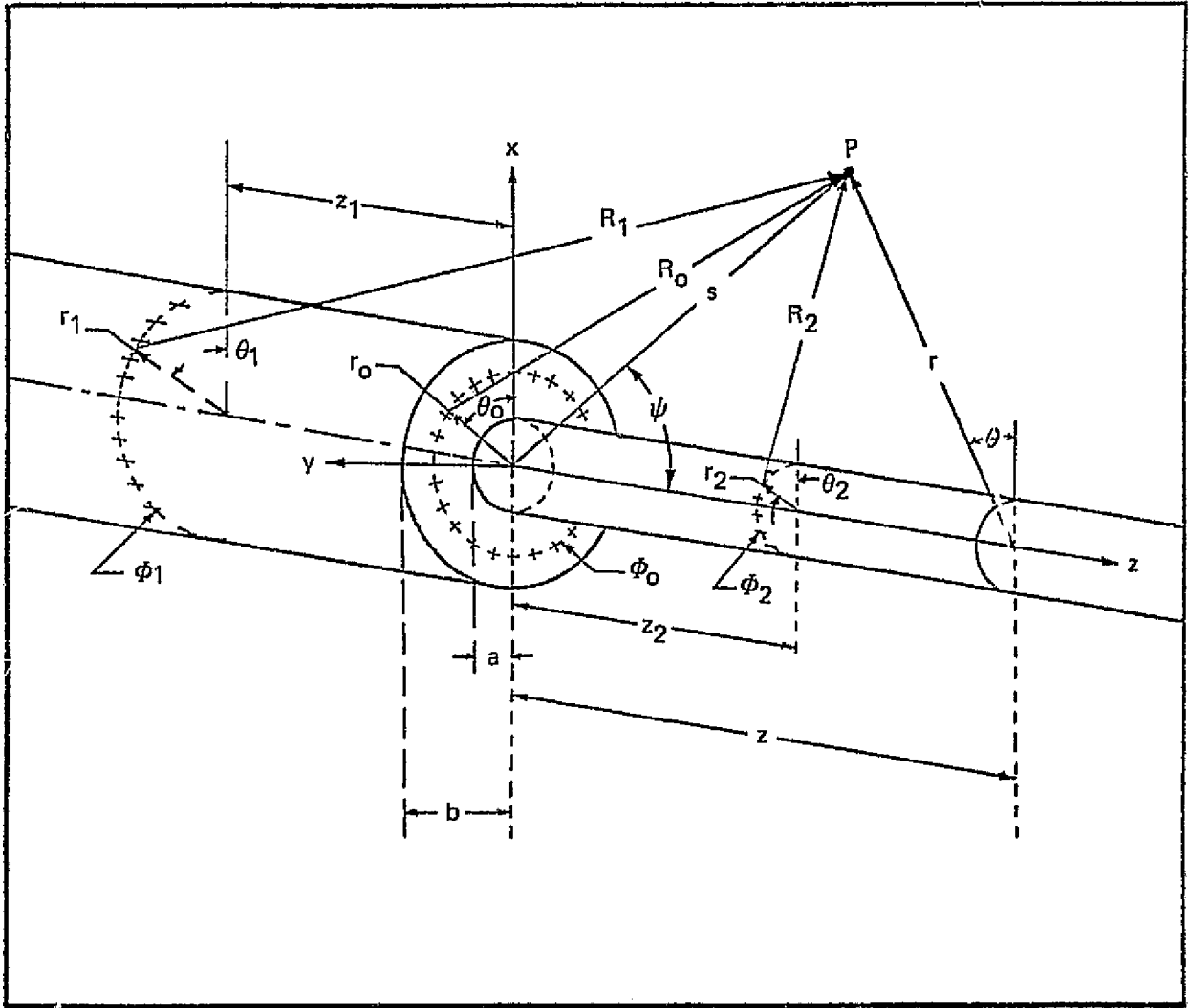
7.0 FIGURES

PRECEDING PAGE BLANK NOT FILMED



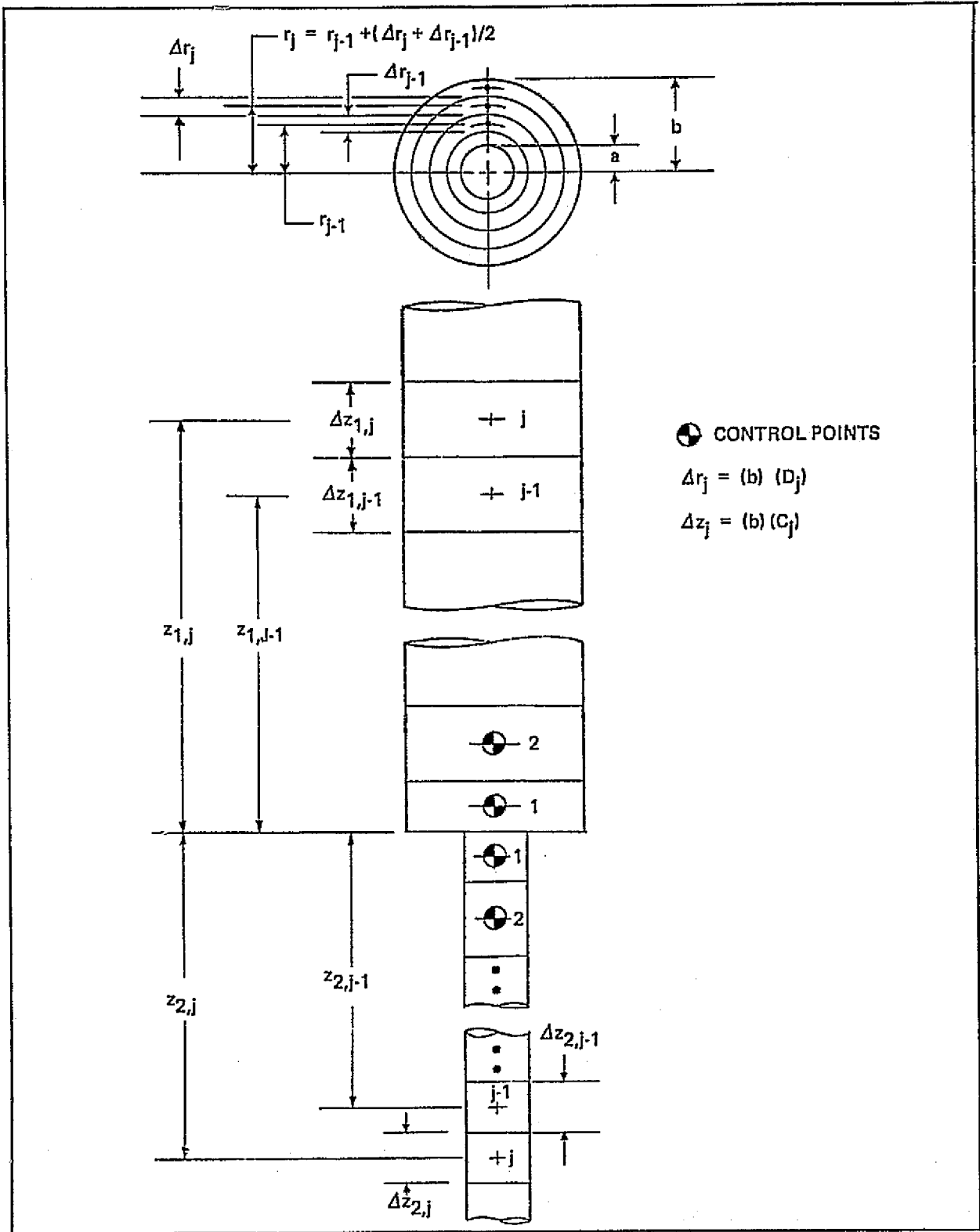
ADMISSIBLE DUCT CONFIGURATIONS  
FIGURE 1

PRECEDING PAGE BLANK NOT FILMED

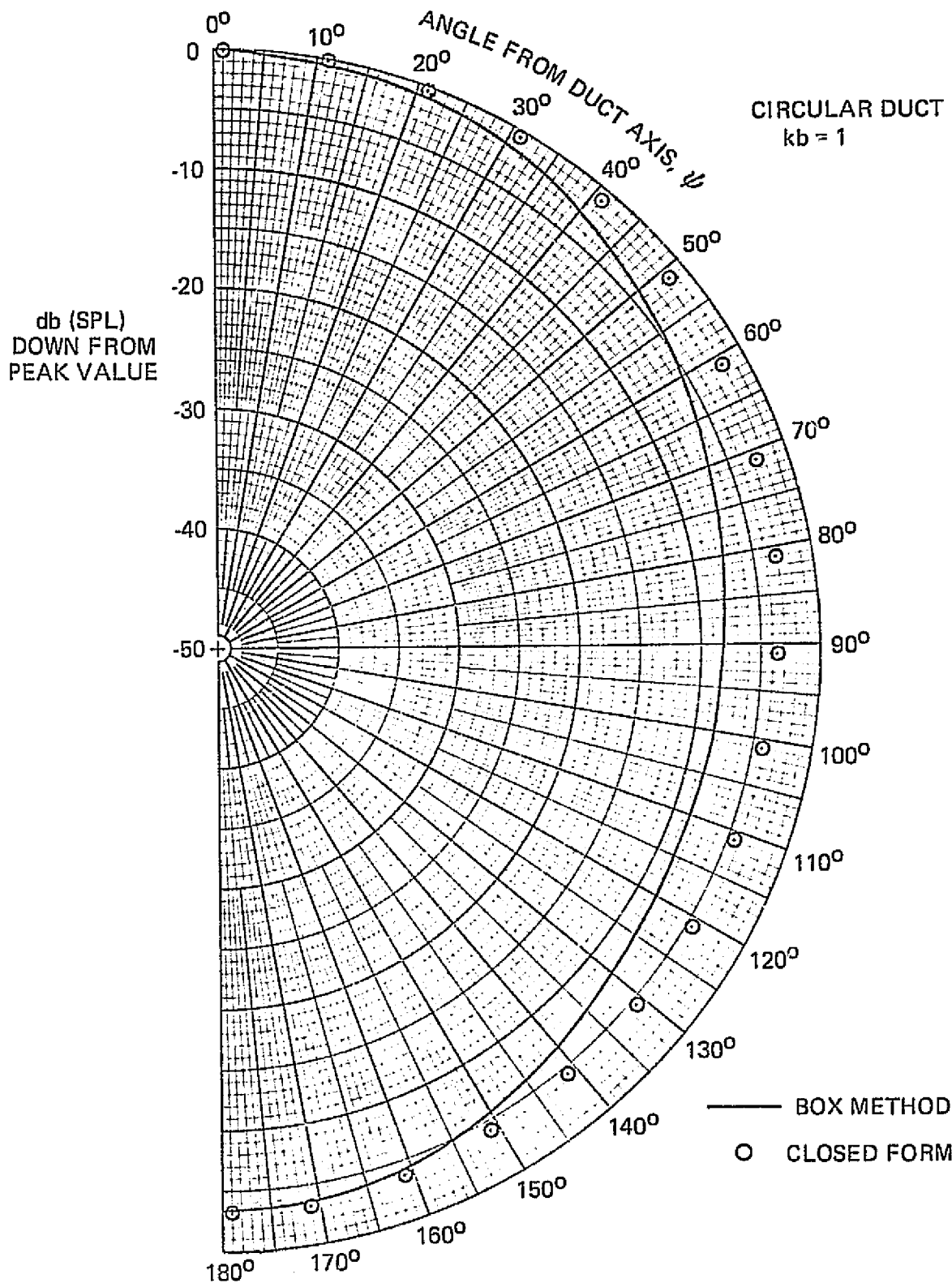


GEOMETRY  
FIGURE 2





BOX METHOD INTEGRATION AND CONTROL BLOCKS  
FIGURE 3



EXAMPLE PROBLEM NORMALIZED DIRECTIVITY PATTERN  
FIGURE 4

**APPENDIX 1**  
**PROGRAM DESCRIPTION**

## NOMENCLATURE

### Computer Program Variables

A	Centerbody Radius
B	Outer Duct Radius
C(I)	Dimensionless Size of Ith Box on Duct Outer Wall
C2(I)	Dimensionless Size of Ith Box on Extended Centerbody Wall
CHK	Convergence Criterion
D(I)	Dimensionless Size of Ith Box on Duct Exit Face
FFR	Far-field radius
G(I)	Directivity function of Ith Polar Angle
GR(I)	Normalized radiation pattern of Ith Polar Angle
INK	Configuration Parameter
K	No. of Polar Angles at which Far-Field Data is required
MW	Angular Mode No.
M	No. of Annular Boxes
N	No. of Cylindrical Boxes on Duct Wall
N2	No. of Cylindrical Boxes on Extended Centerbody Wall
NG	Order of Gaussian Quadrature
PHI(I)	Source Strength Distribution of Ith Box
POP(I)	Polar Angle array in degrees
R	Radial Coordinate
RO, RI	Distance between Point on Duct and Field Point
S	Sound Speed in Air
TT	Angular Coordinate
TI	Angular Coordinate Integration Variable
W	Frequency Radians/Second
WDS	Wavenumber W/S
XANG	Nondimensional Angular Size for Control Box
ZZ	Axial Coordinate

The basic operation of the Directivity Index Computer Program is described and the input/output formats are listed. A flow chart of the program is presented in Appendix 2 and listings of the main program and its subroutines are presented in Appendices 3 thru 5. The input preparation and output format of the program used for the example problem in Section 4.1 is presented in Appendix 6.

## INPUT

The input data for the program consists of 16 variables whose symbols and card formats are described below:

CARD OR CARD SET	FORMAT	DATA
1	3612	K      Number of angular points, $\psi_1$ , at which the directivity index will be calculated
		M      Number of annular rings used to represent the face of the duct
		N      Number of cylindrical rings used to represent the outer duct wall
		N2     Number of cylindrical rings used to represent the extended inner duct wall (if present)
		INK    Indicator for extending the inner duct wall past the duct face. 0 does not extend the wall, 1 extends it to infinity.
		ND     Maximum number of passes to be made through the quadrature iteration loop. ND is related to the highest quadrature order NG by $ND = \frac{NG-2}{2}$
		MW     Angular mode number
2	6E12.6	A      Inner duct radius
		B      Outer duct radius
		W      Circular frequency, radians/second
		S      Speed of sound in units consistent with those of A and B
		CHK    Convergence criteria for numerical integration

CARD OR  
CARD SET FORMAT

DATA

		FFR	Separation Distance
3	6E12.6 I = 1, M	D(I)	Annular ring box widths. These widths are normalized by the outer duct radius, numbered D(1) at the duct centerline (or adjacent to the centerbody wall-duct exit plane intersection/ and I increasing to D(M) at the lip of the duct.
4	6E12.6 I = 1, N	C(I),	Outer duct wall box lengths. These lengths are normalized by the outer duct radius, numbered with C(I) closest to the duct exit plane and I increasing in the negative z direction.
5*	6E12.6 I = 1, N2	C2(I),	Extended centerbody duct wall box lengths. These lengths are normalized by the outer duct radius, numbered with C2(I) closest to the duct exit plane and I increasing in the positive z direction.
6	6E12.6 I = 1, M	PHIO(I),	Source distribution on duct face. Method of numbering this source distribution is analogous to D(I).
7	6E12.6 I = 1, N	PH11(I),	Source distribution on outer duct wall. Method of numbering this source distribution is analogous to C(I).
8*	6E12.6 I = 1, N2	PH12(I),	Source distribution on extended centerbody wall. Method of numbering this source distribution is analogous to C2(I).

\* Card Sets 5 and 8 are needed only if INK = 1

#### PROGRAM FLOW

Program operation consists of two basic loops, one of which calculates the directivity function and the other which determines the normalized radiation pattern. An initial value of the angle  $\psi$  is calculated. Equations (14) through (16) are solved to yield the exit plane and duct wall contributions  $G_1, G_2, G_3$  to the far-field directivity function. The maximum absolute value of the directivity function  $G$  is found and used to calculate the normalized radiation pattern as follows:

$$GR = 20 \log_{10} \left( \frac{G}{G_{\max}} \right)$$

Calculation of the directivity function requires two subroutines, GAUSS and BESJY. GAUSS is the subroutine that provides the weights and abscissae for the Gaussian quadrature described in Equation (14). BESJY supplies the value of the Bessel function  $J_m$  for the argument XARG. Listings of GAUSS and BESJY are presented in Appendices 4 and 5, respectively.

## OUTPUT

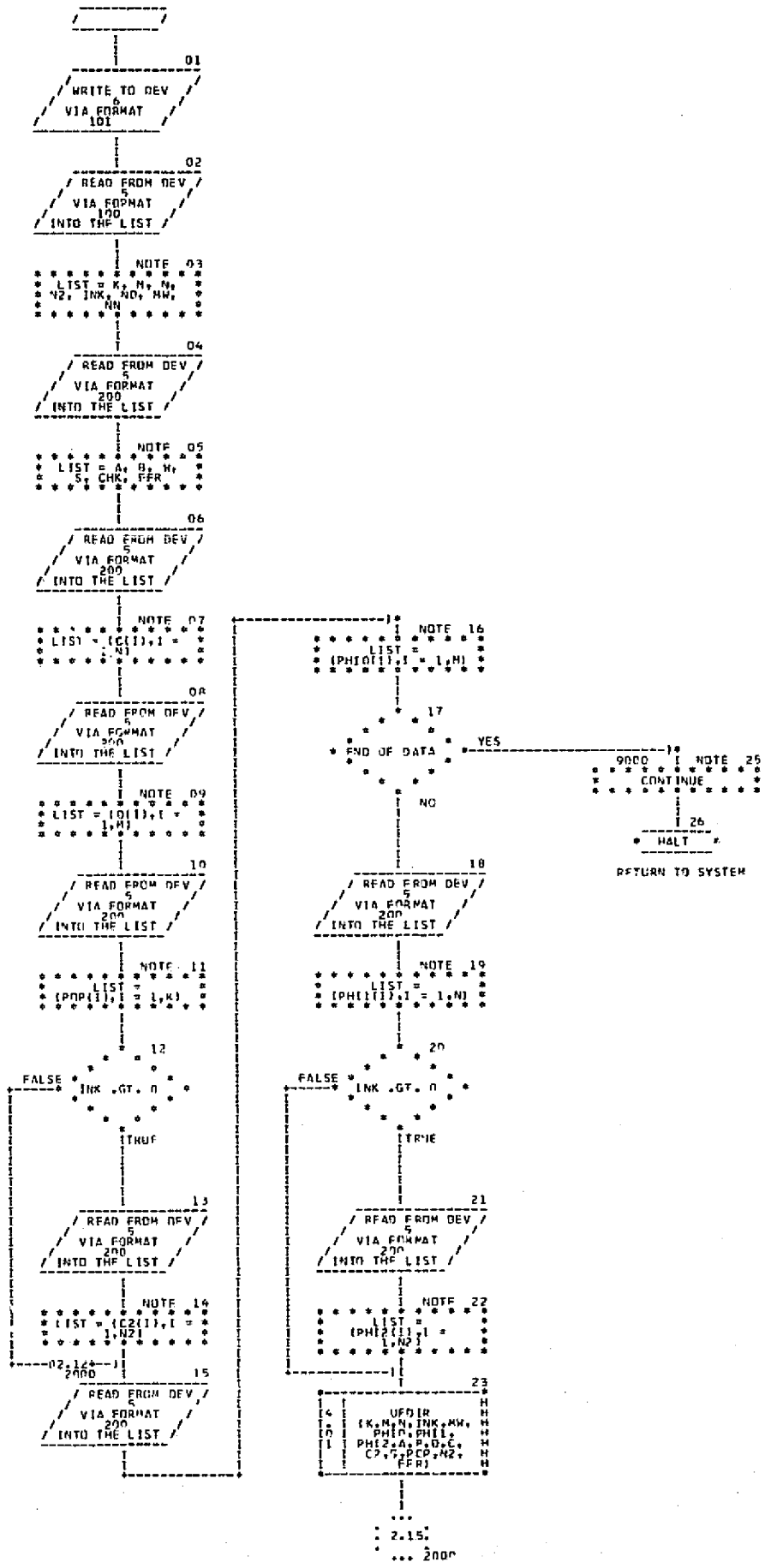
The output format consists of three groups of data:

- Input Data – All pertinent input data are printed out.
- Directivity Function – The directivity function array and its associated array of angles,  $\psi$ , in degrees, are printed out in column format.
- Radiation Pattern – The normalized radiation pattern array and its associated array of angles,  $\psi$ , in degrees, are printed out in column format.

APPENDIX 2  
PROGRAM FLOW CHARTS

**PRECEDING PAGE BLANK NOT FILMED**





02.23---1\*  
 DIRECTIVITY FACTOR -  
 UFBIR  
 ZOMD15 06 - 06  
 X(INO, WT(INDI,  
 XAR(INO), GR(K),  
 G(K)

15 | 01  
 KP = K

20 | 02  
 NOTE  
 CONTINUE

03  
 AF = AD  
 BF = BD

04  
 WRITE TO DEV  
 VIA FORMAT  
 1400  
 FROM THE LIST

05  
 WRITE TO DEV  
 VIA FORMAT  
 1000  
 FROM THE LIST

06  
 NOTE  
 LIST = K, MW

07  
 WRITE TO DEV  
 VIA FORMAT  
 1000  
 FROM THE LIST

08  
 NOTE  
 LIST = M, N, N2,

09  
 WRITE TO DEV  
 VIA FORMAT  
 1070  
 FROM THE LIST

10  
 NOTE  
 LIST = INK

11  
 WRITE TO DEV  
 VIA FORMAT  
 1000  
 FROM THE LIST

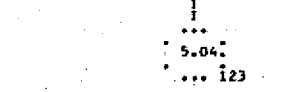
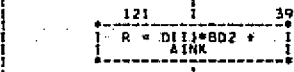
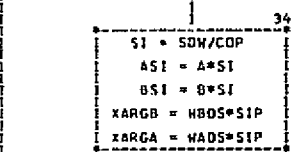
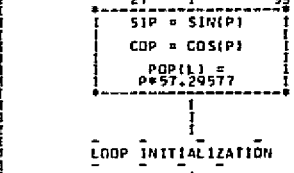
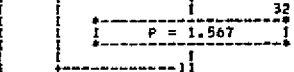
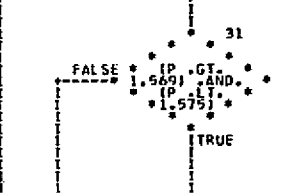
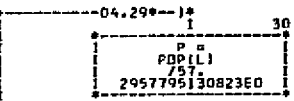
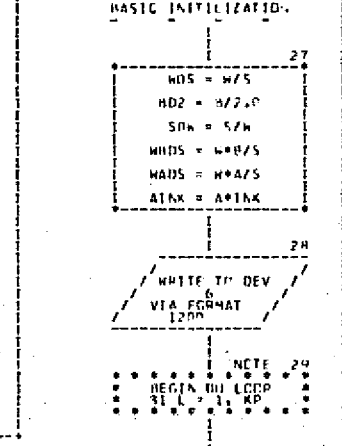
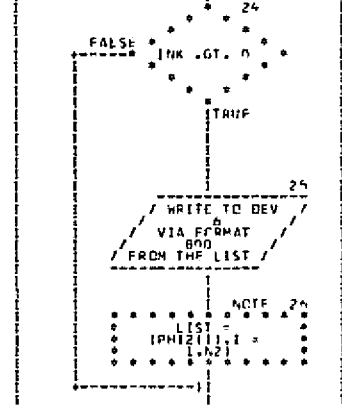
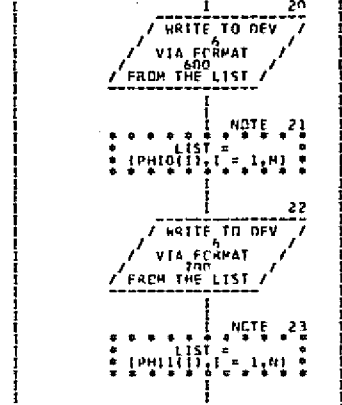
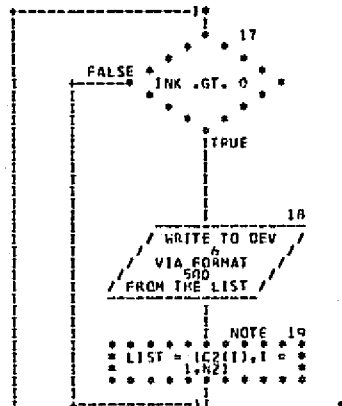
12  
 NOTE  
 LIST = A, A, W,  
 S, CHK

13  
 WRITE TO DEV  
 VIA FORMAT  
 700  
 FROM THE LIST

14  
 NOTE  
 LIST = (O(I), I =

15  
 WRITE TO DEV  
 VIA FORMAT  
 400  
 FROM THE LIST

NOTE  
 LIST = (C(I), I =



```

04.30---1
      03
      11 = 1 - 1
      R = R + (D(I)) +
      D(I)*D(I)
04.30---1
      123
      04
      X1 = (0,0,0,0)
      DD20 = DD2*B(I)
  
```

NO IS THE HIGEST ORDER GAUSSIAN QUAD USED.

```

***** NLTF 05
***** BEGIN DO LOOP
***** 150 KK = 1, NO
*****
05.19---1
      06
  
```

```

      ILK = KK
      ILL = NN +
      2*IKK - 1
  
```

```

      GAUSS
      (X,MT,ILL)
  
```

```

      XAR(KK) =
      (0,0,0,0)
      YAR = 0,0
  
```

```

***** NOTE 09
***** BEGIN DO LOOP
***** 155 I1 = 1, ILL
*****
  
```

```

      I1 = I1 -
      DD20*X(I1)
      XARG = R(I1)*D(I1)
  
```

```

***** HFSJY
***** (XARG, MT, I1,
***** DUM, DUM, DUM,
***** I, R)
  
```

```

      YAR = YAR +
      R(I1)*D(I1)
  
```

```

***** END OF DO
***** LOOP
      YES
  
```

```

      XAR(KK) =
      GABL(X,YAR,D(I1)
      *D(I1))
  
```

```

      KL = KK - 1
      ALT =
      ABS(CABS(XAR(KK))
      - CABS(XAR(KL)))
  
```

```

      KK = >
  
```

```

      AMT = CHK
  
```

```

      150
  
```

```

      157
  
```

```

05.15---1
      157
      16
      KK = NO
      (0)
      01
      158
  
```

WRITE 1<sup>ST</sup> DEV VIA FORMAT 1030 FROM THE LIST

```

***** NOTE 18
***** LIST = AMT, CHK,
***** R
  
```

```

05.02---1
      150
      19
      END OF DO
      LOOP
      YES
  
```

```

***** NOTE 20
***** 160
***** CONTINUE
  
```

```

      X1 = X1 +
      XAR(I1,K)
  
```

```

      G1 = G1 +
      X1*PHI(I1)
  
```

```

***** END OF DO
***** LOOP
      YES
  
```

```

      COMPUTE CONTRIBUTION
      OF OUTER RULI WALL
  
```

```

      G2 = (0,0,0,0)
  
```

```

***** NOTE 25
***** BEGIN DO LOOP
***** 200 I = 1, N
*****
06.25---1
      20
  
```

```

      I = 1
  
```

```

      200
  
```

```

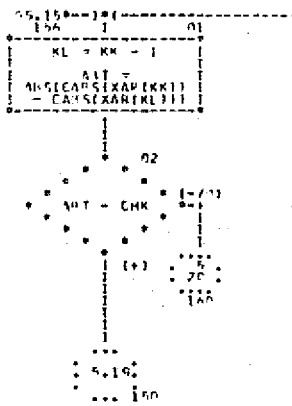
      221
      22 = E(I)*D(I)
  
```

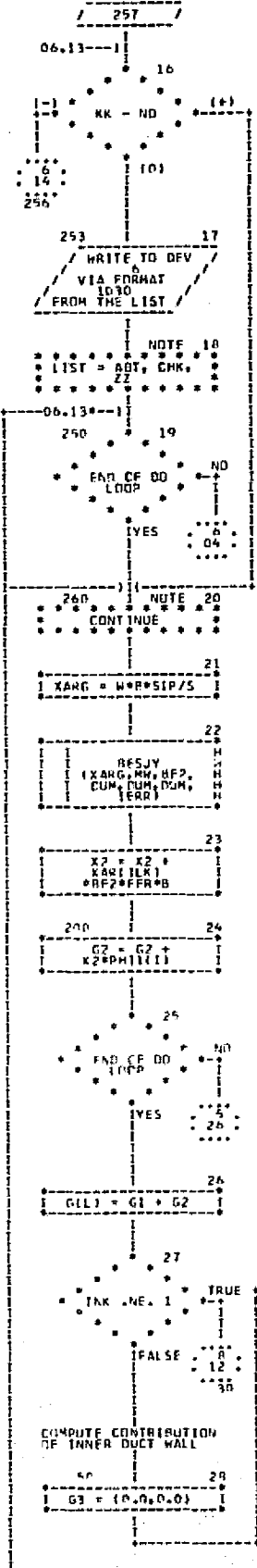
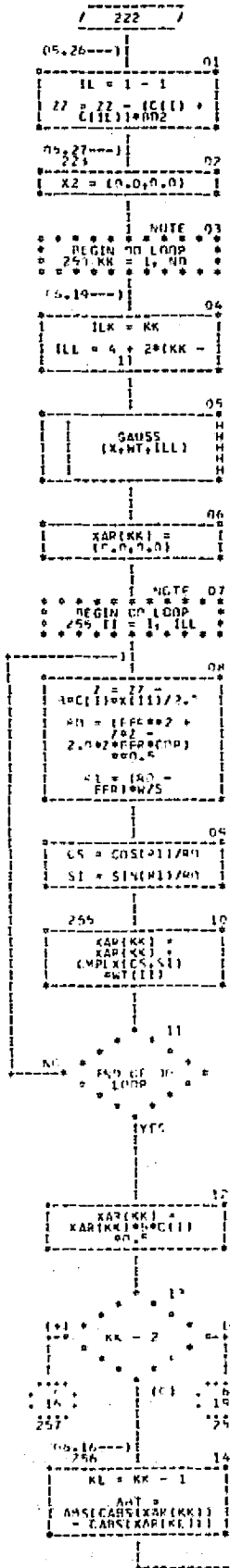
```

      22
  
```

```

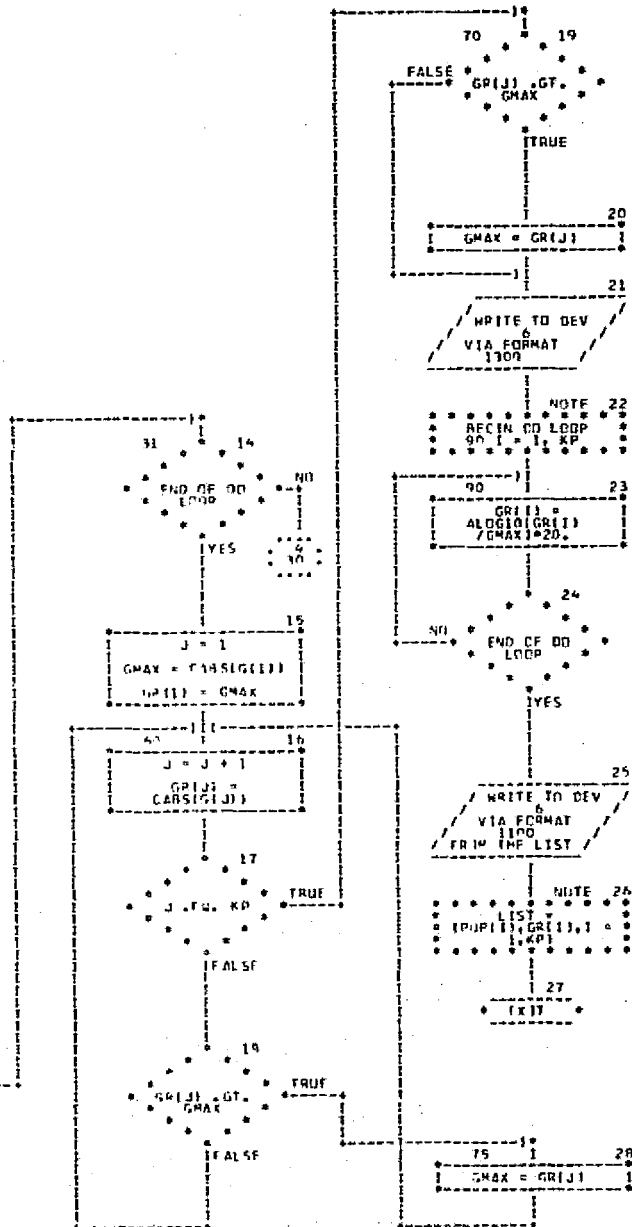
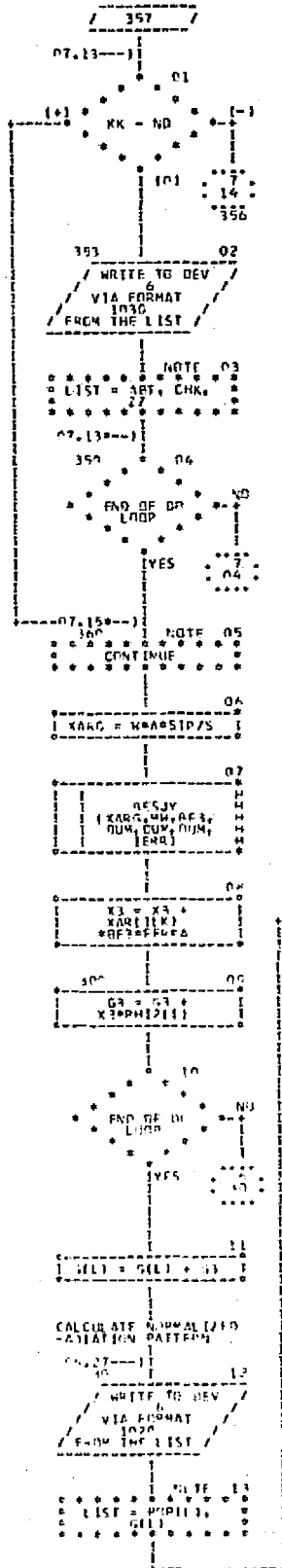
      223
  
```





ORIGINAL PAGE IS OF POOR QUALITY





ORIGINAL PAGE IS  
OF POOR QUALITY

APPENDIX 3  
MAIN PROGRAM LISTING

PRECEDING PAGE BLANK NOT FILMED

```

C   NEW   DIRECTIVITY INDEX PROGRAM
      DIMENSION C(40), POP(180) , D(40) , C2(40)
      COMPLEX *08
      1    PHIO(40), PHI1(40), PHI2(40), G(180)
      COMMON /GEN/  W, S, CHK, NN, ND
100  FORMAT(36I2)
200  FORMAT(6F12.6)
101  FORMAT ('1 ENTERING THE DIRECTIVITY FACTOR PROGRAM.'//)

C   *   *   *   *   *   *   *   *   *   *   *   *   *
C
      WRITE (6,101)
      READ (5,100)  K, M, N, N2, INK, ND, MW, NN
      READ (5,200)  A, B, W, S, CHK, FFR
      READ (5,200)  (C(I),I=1,N)
      READ (5,200)  (D(I),I=1,M)
      READ (5,200)  (POP(I),I=1,K)
      IF (INK .GT. 0) READ (5,200) (C2(I),I=1,N2)
2000 READ(5,200 ,END=9000) (PHIO(I),I=1,M)
      READ (5,200)  (PHI1(I),I=1,N)
      IF (INK .GT. 0) READ (5,200) (PHI2(I),I=1,N2)
      CALL UFDIR (K ,M, N, INK, MW, PHIO, PHI1, PHI2, A ,B ,D, C, C2,G
1      ,POP, N2, FFR)
                                           GO TO 2000

9000 CONTINUE
      STOP
      END

```



```

SUBROUTINE UFDIR
1      (K ,M, N, INK, MW, PHIO, PHI1, PHI2, AD,BD,D, C, C2,G
2      ,POP, N2, FFR )
C      DIRECTIVITY FACTOR - UFDIR                ZDM915 06 - 06
REAL *8 AD, BD
C      X(ND, WT(ND), XAR(ND), GR(K), G(K)
DIMENSION C(1 ),X(20) ,WT(20),POP(1 ),GR(170),D(1) ,C2(1)
COMPLEX *08
1      PHIO(1), PHI1(1), PHI2(1), XAR(20),
2      G1, G2, G3,X1,X2,X3,G(180),DMPLX
COMMON /GFN/ W, S, CHK, NN, ND
EQUIVALENCE (A,AE),(B,BE)
C
330 FORMAT ('O ANNULAR RING BOX WIDTHS'/(8X1P4E15.4))
400 FORMAT ('O OUTER DUCT WALL BOX LENGTHS'/(8X1P4E15.4))
500 FORMAT ('O INNER DUCT WALL BOX LENGTHS'/(8X1P4E15.4))
600 FORMAT ('O SOURCE DISTRIBUTION ON DUCT FACE.'/(8X1P4E15.4))
700 FORMAT ('O SOURCE DISTRIBUTION ON OUTER DUCT WALL.'/(8X1P4E15.4))
800 FORMAT ('O SOURCE DISTRIBUTION ON INNER DUCT WALL.'/(8X1P4E15.4))
1000 FORMAT(36I2)
1010 FORMAT(6E12.6)
1020 FORMAT(' P (IN DEGREES) =', F13.5,10X'G =',2E13.5)
1030 FORMAT (' ** INTEGRATION DID NOT CONVERGE. DIFFERENCE =',
1 F10.4, ' CHK =',F10.4, ' R =',F10.4)

1050 FORMAT(1H ,10X,'NUMBER OF PSI POINTS =',I5,5X,'ANGULAR MODE',
1' NUMBER =',I5)
1060 FORMAT (1H ,10X, 'NUMBER OF ANNULAR RING SEGMENTS =', I5/11X
1 , 'NUMBER OF OUTER DUCT WALL SEGMENTS =', I5/11X, 'NUMBER OF'
2 , ' INNER DUCT WALL SEGMENTS =', I5/11X, 'HIGHEST ORDER GAUSS'
3 , 'IAN QUADRATURE =',I5)
1070 FORMAT(1H ,10X,'IS INNER DUCT PRESENT 0=NO,1=YES ',I5)
1080 FORMAT(1H ,10X,'DUCT OR =',F10.4,'FT',5X,'DUCT IR =',F10.4,
1'FT',/,5X,'FREQUENCY =',F10.4,' RAD/SEC',5X,'SPEED OF SOUND=',
2F10.4,2X,'FT/SEC',/,5X,'INTEGRATION CONVERGENCE NO =',F10.4)
1100 FORMAT(' P (IN DEGREES) =', F13.5,10X, 'SPL =', F13.5)
1200 FORMAT ('1',25X,'D I R E C T I V I T Y F U N C T I O N'//)
1300 FORMAT ('1',25X,'R A D I A T I O N P A T T E R N'//)
1400 FORMAT ('1',25X,'I N P U T D A T A'//)
C
C * * * * *
5577 FORMAT ('C $UFDIR$ ', 8G15.7/ (10X,8G15.7))
C
15 KP = K
20 CONTINUE
AF = AD
BE = BD
WRITE (6,1400)
WRITE(6,1050) K,MW
WRITE(6,1060) M,N,N2, ND
WRITE(6,1070) INK

```

```

WRITE(6,1080) B,A,W,S,CHK
WRITE (6,330) ( D(I),I=1,M)
WRITE (6,400) ( C(I),I=1,N)
IF(INK .GT. 0) WRITE (6,500) (C2(I),I=1,N2)
WRITE (6,600) (PHIO(I),I=1,M)
WRITE (6,700) (PHI1(I),I=1,N)
IF (INK. GT. C) WRITE (6,800) (PHI2(I),I=1,N2)
C - - - BASIC INITILIZATION - - -
WDS = W / S
RD2 = B / 2.0
SDW = S / W
WBDS = W * B / S
WADS = W * A / S
AINK = A * INK
WRITE (6,1200)
DO 31 L=1,KP
P = POP(L) / 57.2957795130823E0
IF((P.GT.1.569).AND.(P.LT.1.575)) P= 1.567
27 SIP = SIN(P)
COP = COS(P)
POP(L)=P*57.29577
C - - - LOOP INITIALIZATION - - -
SI = SDW / COP
ASI = A * SI
BSI = B * SI
XARGB = WRDS * SIP
XARGA = WADS * SIP
WDSSIP = WDS * SIP
C
C COMPUTE CONTRIBLTION OF DUCT FACE
C
G1 = (0.0,0.0)
DO 100 I=1,M
IF(I-1) 121,121,122
121 R = D(I)*RD2 + A INK
GO TO 123
122 IL = I-1
R = R + (D(I)+D(IL))*RD2
123 X1 = (0.0,0.0)
BD2D = BD2 * D(I)
C ND IS THE HIGEST ORDER GAUSSIAN QUAD USED.
DO 150 KK=1,ND
ILK = KK
ILL =NN+2*(KK-1)
CALL GALSS(X,WT,ILL)
XAR(KK) = (0.0,0.0)
YAR = 0.0
DO 155 II=1,ILL
RO = R - BD2D *X(II)
XARG = RO* WDSSIP
CALL BESJY(XARG, MW, BFI, DUM, DUM, DUM, IERR)

```

```

155 YAR = YAR+BF1*RO * WT{II}
    XAR(KK) = CMLX {YAR*B * P{I} *.5, 0.0E0}
    IF(KK-2) 150,156,157
156 KL = KK-1
    ABT = ABS(C ABS(XAR(KK)) - C ABS(XAR(KL)))
    IF(ABT-CHK) 160,160,150
157 IF(KK-ND) 156,153,160
153 WRITE (6,1030) ABT, CHK, R
150 CONTINUE
160 CONTINUE
    X1 = X1 + XAR(ILK)
100 G1 = G1+X1*PHIO(I)
C
C   COMPUTE CONTRIBUTION OF OUTER DUCT WALL
C
    G2 = {0.C,0.0}
    DO 200 I=1,N
    IF(I-1) 221,221,222
221 ZZ = -C(I)*BD2
    GO TO 223
222 IL = I-1
    ZZ = ZZ-(C(I)+C(IL))*BD2
223 X2={0.C,C.0}
    DO 250 KK=1,ND
    ILK=KK
    ILL=4+2*(KK-1)
    CALL GAUSS(X,WT,ILL)
    XAR(KK)={0.0,0.C}
    DO 255 II=1,ILL
    Z=ZZ-B*C(I)*X(II)/2.C
    RO=(FFR**2+Z*Z-2.0*7*FFR*CDP)**0.5
    RI=(RO-FFR)*W/S
    CS=COS(RI)/RO
    SI=SIN(RI)/RO
255 XAR(KK)=XAR(KK)+CMLX(CS,SI)*WT{II}
    XAR(KK)=XAR(KK)*B*C(I)*0.5
    IF(KK-2) 250,256,257
256 KL=KK-1
    ABT=ABS(CABS(XAR(KK))-CABS(XAR(KL)))
    IF(ABT-CHK) 260,260,250
257 IF(KK-ND) 256,253,260
253 WRITE(6,1030) ABT,CHK,ZZ
250 CONTINUE
260 CONTINUE
    XARG=W*B*SI*P/S
    CALL BESJY (XARG, MW, BF2, DUM, DUM, DUM, IFRR)
    X2=X2+XAR(ILK)*BF2*FFR*B
200 G2=G2+X2*PHI1(I)
C
    G(L) = G1 + G2
    IF (INK .NE. 1)

```

```

C
C      COMPUTE CONTRIBUTION OF INNER DUCT WALL
C
50 G3 = (0.0,0.0)
   DO 300 I=1,N2
     IF(I-1) 321, 321, 322
321 ZZ=C2(I)*R/2.0
     GO TO 323
322 IL = I-1
     ZZ=ZZ+(C2(I)+C2(IL))*R/2.0
323 X3=(0.0,0.0)
     DO 350 KK=1,ND
       ILK=KK
       ILL=4+2*(KK-1)
       CALL GAUSS(X,WT,ILL)
       XAR(KK)=(0.0,0.0)
       DO 355 II=1,ILL
         Z=77+R*C2(I)*X(II)/2.0
         RO=(FFR**2+Z*Z-2.0*Z*FFR*COF)**0.5
         RI=(RO-FFR)*W/S
         CS=COS(RI)/RO
         SI=SIN(RI)/RO
355 XAR(KK)=XAR(KK)+CMPLX(CS,SI)*WT(II)
         XAR(KK)=XAR(KK)*R*C2(I)*0.5
         IF(KK-2) 350,356,357
356 KL=KK-1
         ABT=ABS(CABS(XAR(KK))-CABS(XAR(KL)))
         IF(ABT-CHK)360,360,350
357 IF(KK-ND) 356,353,360
353 WRITE(6,1030) ABT,CHK,ZZ
350 CONTINUE
360 CONTINUE
     XARG=W*A*SIP/S
     CALL BESJY (XARG, MW, BF3, DUM, DUM, DUM, IERR)
     X3=X3+XAR(ILK)*BF3*FFR*A
300 G3=G3+X3*PHI2(I)
     G(L) = G(L) + G3

C
C      CALCULATE NORMALIZED RADIATION PATTERN
C
30 WRITE(6,1020) POP(L),G(L)
31 CONTINUE
   J=1
   GMAX = C ABS(G(1))
   GR(1)=GMAX
60 J=J+1
   GR(J) = C ABS(G(J))
   IF(J.EQ.KP) GO TO 70
   IF(GR(J).GT.GMAX) GO TO 75
   GO TO 60
75 GMAX=GR(J)

```

```
GO TO 6C
70 IF(GR(J).GT.GMAX) GMAX=GR(J)
WRITE (6,1300)
DO 90 I=1,KP
90 GR(I)=ALOG10(GR(I)/GMAX)*20.
WRITE(6,1100){POP(I),GR(I) ,I=1,KP}
RETURN
END
```

APPENDIX 4  
GAUSS SUBROUTINE LISTING

~~PRECEDING PAGE BLANK NOT FILMED~~

```

SUBROUTINE GAUSS(X,WT,M)
  STORE DP TEST IN 81
  IMPLICIT REAL*8 (A-H,O-Z)
  DIMENSION X(12),WT(12)
  IF(M-4)10,11,12
10 X(1)=-0.577350269189626
   X(2)=-X(1)
   WT(1)=1.0
   WT(2)=1.0
   GO TO 20
11 X(1)=-0.861136311594053
   X(2)=-0.339981043584856
   X(3)=-X(2)
   X(4)=-X(1)
   WT(1)=0.347854845137454
   WT(2)=0.652145154862546
   WT(3)=WT(2)
   WT(4)=WT(1)
   GO TO 20
12 IF(M-8)13,14,15
13 X(1)=-0.932469514203152
   X(2)=-0.661209386466265
   X(3)=-0.238619186083197
   X(4)=-X(3)
   X(5)=-X(2)
   X(6)=-X(1)
   WT(1)=0.171324492379170
   WT(2)=0.360761573048139
   WT(3)=0.467913934572691
   WT(4)=WT(3)
   WT(5)=WT(2)
   WT(6)=WT(1)
   GO TO 20
14 X(1)=-0.960289856497536
   X(2)=-0.796666477413627
   X(3)=-0.525532409916329
   X(4)=-0.183434642495650
   X(5)=-X(4)
   X(6)=-X(3)
   X(7)=-X(2)
   X(8)=-X(1)
   WT(1)=0.101228536290376
   WT(2)=0.222381034453374
   WT(3)=0.313706645877887
   WT(4)=0.362683783378362
   WT(5)=WT(4)
   WT(6)=WT(3)
   WT(7)=WT(2)
   WT(8)=WT(1)
   GO TO 20
15 IF(M-12)16,17,18

```

ZDM915 11 - BT

```

16 X(1)=-0.973906528517172
   X(2)=-0.865063366688985
   X(3)=-0.679409568299024
   X(4)=-0.433395394129247
   X(5)=-0.148874338981631
   X(6)=-      X(5)
   X(7)=-      X(4)
   X(8)=-      X(3)
   X(9)=-      X(2)
   X(10)=-     X(1)
   WT(1)=0.066671344308688
   WT(2)=0.149451349150581
   WT(3)=0.219086362515982
   WT(4)=0.269266719309996
   WT(5)=0.295524224714753
   WT(6)=WT(5)
   WT(7)=WT(4)
   WT(8)=WT(3)
   WT(9)=WT(2)
   WT(10)=WT(1)
   GO TO 20

```

```

17 X(1)=-0.981560634246719
   X(2)=-0.904117256370475
   X(3)=-0.769902674194305
   X(4)=-0.587317954286617
   X(5)=-0.367831498918180
   X(6)=-0.125333408511469
   X(7)=-      X(6)
   X(8)=-      X(5)
   X(9)=-      X(4)
   X(10)=-     X(3)
   X(11)=-     X(2)
   X(12)=-     X(1)
   WT(1)=0.047175336386512
   WT(2)=0.106939325995318
   WT(3)=0.160078328543346
   WT(4)=0.203167426723066
   WT(5)=0.233492536538355
   WT(6)=0.249147045813403
   WT(7)=WT(6)
   WT(8)=WT(5)
   WT(9)=WT(4)
   WT(10)=WT(3)
   WT(11)=WT(2)
   WT(12)=WT(1)

```

```

18   IF (M-16)
19 X(1)=-0.986283808696812
   X(2)=-0.928434883663574
   X(3)=-0.827201315069765
   X(4)=-0.687292904811685

```

19, 21, 20

GO TO 20



X(5)=-0.515248636358154  
 X(6)=-0.319112368927890  
 X(7)=-0.108054948707344  
 X(8)=- X(7)  
 X(9)=- X(6)  
 X(10)= -X(5)  
 X(11)=- X(4)  
 X(12)=- X(3)  
 X(13)=- X(2)  
 X(14)=- X(1)  
 WT(1)=0.035119460331752  
 WT(2)=C.080158087159760  
 WT(3)=0.121518570687903  
 WT(4)=0.157203167158194  
 WT(5)=0.185538397477938  
 WT(6)=0.205198463721296  
 WT(7)=0.215263853463158  
 WT(8)=WT(7)  
 WT(9)=WT(6)  
 WT(10)=WT(5)  
 WT(11)=WT(4)  
 WT(12)=WT(3)  
 WT(13)=WT(2)  
 WT(14)=WT(1)

GO TO 20

21 X(1)=-0.989400934991650  
 X(2)=-0.944575023073233  
 X(3)=-C.865631202387832  
 X(4)=-0.755404408355003  
 X(5)=-0.617876244402644  
 X(6)=-0.458016777657227  
 X(7)=-0.281603550779259  
 X(8)=-0.095012509837637  
 X(9)=- X(8)  
 X(10)= -X(7)  
 X(11)=- X(6)  
 X(12)=- X(5)  
 X(13)=- X(4)  
 X(14)=- X(3)  
 X(15)=- X(2)  
 X(16)=- X(1)  
 WT(1)=0.027152459411754  
 WT(2)=0.062253523938648  
 WT(3)=0.095158511682493  
 WT(4)=0.124628971255534  
 WT(5)=0.149595988816577  
 WT(6)=0.169156519395003  
 WT(7)=0.182603415044924  
 WT(8)=0.189450610455069  
 WT(9)=WT(8)  
 WT(10)=WT(7)

```
WT(11)=WT(6)
WT(12)=WT(5)
WT(13)=WT(4)
WT(14)=WT(3)
WT(15)=WT(2)
WT(16)=WT(1)
20 RETURN
END
```

APPENDIX 5  
BESJY SUBROUTINE LISTING

PRECEDING PAGE BLANK NOT FILMED.

```

SUBROUTINE BESJY(X,NO,BJ,BY,BJJ,BYY,IERR)
REAL J(350),J0,J1,J00
DIMENSION Y(80)
PI=3.141593
IF(X.GT.0.) GO TO 90
IERR=0
GO TO 80
90 CONTINUE
IERR=1
FAC = 1.5
      IF (X .GT. 50.0)          FAC = 0.5
NX=3.9+FAC*X+NO
J(2*NX+2)=0.
J(2*NX+1)=1.E-29
C=0.
J0=0.
J1=0.
Y0=0.
Y1=0.
DO 20 NB=1,NX
N=NX+1-NB
RN=N
J(2*N)=2.*(2.*RN+1)*J(2*N+1)/X-J(2*N+2)
J(2*N-1)=4.*RN*J(2*N)/X-J(2*N+1)
Y0=Y0+(-1)**N*J(2*N)/RN
Y1=Y1+(-1)**N*(2*RN+1.)*J(2*N+1)/RN/(1.+RN)
20 C=C+2.*J(2*N)
J00=2.*J(1)/X-J(2)
C=J00+C
Y0=(ALOG(X/2.)+.57721566)*J00-2.*Y0
Y1=(ALOG(X/2.)-.42278434)*J(1)-J00/X-Y1
Y0=.6366198*Y0/C
Y1=.6366198*Y1/C
J0=J00/C
Y(1)=Y1
Y(2)=2.*Y(1)/X-Y0
NNX=NO+2
DO 30 I=1,NNX
Y(I+2)=2.*FLOAT(I+1)*Y(I+1)/X-Y(I)
30 J(I)=J(I)/C
IF(NO.EQ.0) GOT O 70
BJ=J(NO)
BY=Y(NO)
NP=NO+1
BJJ=J(NP)
BYY=Y(NP)
GO TO 80
70 BJ=J0
BY=Y0
BJJ=J(1)
BYY=Y(1)
80 CONTINUE
RETURN
END

```

**APPENDIX 6**  
**EXAMPLE PROBLEM**

8916400000080C 230 8

	1.0	343.0	343.0	.0001	100.
2.500000-02	2.500000-02	5.000000-02	5.000000-02	5.000000-02	5.000000-02
7.500000-02	7.500000-02	7.500000-02	7.500000-02	7.500000-02	7.500000-02
1.000000-01	1.000000-01	1.000000-01	1.000000-01	1.000000-01	1.000000-01
1.000000-01	1.000000-01	1.000000-01	1.250000-01	1.250000-01	1.250000-01
1.250000-01	1.250000-01	1.250000-01	1.250000-01	1.250000-01	1.250000-01
1.250000-01	1.250000-01	1.250000-01	1.250000-01	1.250000-01	1.500000-01
1.500000-01	1.500000-01	1.500000-01	1.500000-01		
1.250000-01	1.250000-01	1.000000-01	7.500000-02	5.000000-02	2.500000-02
2.500000-02	5.000000-02	5.000000-02	7.500000-02	7.500000-02	7.500000-02
5.000000-02	5.000000-02	2.500000-02	2.500000-02		

2.0	4.0	6.0	8.0	10.0	12.0
14.0	16.0	18.0	20.0	22.0	24.0
26.0	28.0	30.0	32.0	34.0	36.0
38.0	40.0	42.0	44.0	46.0	48.0
50.0	52.0	54.0	56.0	58.0	60.0
62.0	64.0	66.0	68.0	70.0	72.0
74.0	76.0	78.0	80.0	82.0	84.0
86.0	88.0	90.0	92.0	94.0	96.0
98.0	100.0	102.0	104.0	106.0	108.0
110.0	112.0	114.0	116.0	118.0	120.0
122.0	124.0	126.0	128.0	130.0	132.0
134.0	136.0	138.0	140.0	142.0	144.0
146.0	148.0	150.0	152.0	154.0	156.0
158.0	160.0	162.0	164.0	166.0	168.0
170.0	172.0	174.0	176.0	178.0	

-6.051150-02	4.396280-02	-7.070610-02	4.862960-02	-9.074880-02	5.779730-02
-1.164650-01	6.955110-02	-1.427180-01	8.154490-02	-1.627780-01	9.070810-02
-1.784120-01	9.784920-02	-2.060100-01	1.104570-01	-2.527120-01	1.317960-01
-3.338090-01	1.688750-01	-4.855940-01	2.383490-01	-7.459170-01	3.576790-01
-1.101920 00	5.209690-01	-1.360750 00	6.385830-01	-1.684620-01	8.127090-02
9.232320 00	-4.792080 00				
-5.246290 01	2.439520 01	3.305650 00	-1.525480 00	9.598000 00	-4.440850 00
6.309650 00	-2.905790 00	3.517480 00	-1.605960 00	1.942270 00	-8.739000-01
9.675640-01	-4.221780-01	4.561170-01	-1.866000-01	2.335750-01	-8.533070-02
1.247160-01	-3.677370-02	6.554990-02	-1.116980-02	3.098380-02	3.159380-03
7.029190-03	1.244690-02	-8.372440-03	1.768620-02	-1.633480-02	1.967140-02
-2.006600-02	1.987230-02	-2.134450-02	1.908200-02	-2.119720-02	1.774860-02
-2.024560-02	1.615220-02	-1.890140-02	1.446720-02	-1.740920-02	1.280810-02
-1.570470-02	1.101020-02	-1.392930-02	9.159830-03	-1.236110-02	7.506910-03
-1.101260-02	6.047700-03	-9.867730-03	4.762740-03	-8.895180-03	3.630740-03
-8.061170-03	2.641050-03	-7.338820-03	1.770590-03	-6.691520-03	1.004170-03
-6.107440-03	3.311800-04	-5.560720-03	-2.687300-04	-5.037840-03	-7.985810-04
-4.531750-03	-1.271280-03	-4.031010-03	-1.701690-03	-3.468190-03	-2.148880-03
-2.825960-03	-2.643200-03	-2.130030-03	-3.230680-03	-1.273980-03	-4.268310-03
3.542770-04	-8.188340-03				

END

I N P U T   D A T A

NUMBER OF PSI POINTS = 89      ANGULAR MODE NUMBER = 0  
 NUMBER OF ANNULAR RING SEGMENTS = 16  
 NUMBER OF OUTER DUCT WALL SEGMENTS = 40  
 NUMBER OF INNER DUCT WALL SEGMENTS = 0  
 HIGHEST ORDER GAUSSIAN QUADRATURE = 8  
 IS INNER DUCT PRESENT 0=NO,1=YES      0  
 DUCT OR = 1.0000FT      DUCT IR = 0.0      FT  
 FREQUENCY = 343.0000 RAD/SEC      SPEED OF SOUND= 343.0000 FT/SEC  
 INTEGRATION CONVERGENCE NO = 0.0001

ANNULAR RING BOX WIDTHS

1.2500E-01	1.2500E-01	1.0000E-01	7.5000E-02
5.0000E-02	2.5000E-02	2.5000E-02	5.0000E-02
5.0000E-02	7.5000E-02	7.5000E-02	7.5000E-02
5.0000E-02	5.0000E-02	2.5000E-02	2.5000E-02

OUTER DUCT WALL BOX LENGTHS

2.5000E-02	2.5000E-02	5.0000E-02	5.0000E-02
5.0000E-02	5.0000E-02	7.5000E-02	7.5000E-02
7.5000E-02	7.5000E-02	7.5000E-02	7.5000E-02
1.0000E-01	1.0000E-01	1.0000E-01	1.0000E-01
1.0000E-01	1.0000E-01	1.0000E-01	1.0000E-01
1.0000E-01	1.2500E-01	1.2500E-01	1.2500E-01
1.2500E-01	1.2500E-01	1.2500E-01	1.2500E-01
1.2500E-01	1.2500E-01	1.2500E-01	1.2500E-01
1.2500E-01	1.2500E-01	1.2500E-01	1.5000E-01
1.5000E-01	1.5000E-01	1.5000E-01	1.5000E-01

SOURCE DISTRIBUTION ON DUCT FACE.

-6.0511E-02	4.3963E-02	-7.0706E-02	4.8630E-02
-9.0749E-02	5.7797E-02	-1.1646E-01	6.9551E-02
-1.4272E-01	8.1545E-02	-1.6278E-01	9.0708E-02
-1.7841E-01	9.7849E-02	-2.0601E-01	1.1046E-01
-2.5271E-01	1.3180E-01	-3.3381E-01	1.6887E-01
-4.8559E-01	2.3835E-01	-7.4592E-01	3.5768E-01
-1.1019E 00	5.2097E-01	-1.3607E 00	6.3858E-01
-1.6846E-01	8.1271E-02	9.2323E 00	-4.2921E 00

SOURCE DISTRIBUTION ON OUTER DUCT WALL.

-5.2463E-01	2.4395E-01	3.3056E-00	-1.5255E-00
9.5980E-00	-4.4408E-00	6.2096E-00	-2.9058E-00
3.5175E-00	-1.606CE-00	1.9423E-00	-8.7390E-01
9.6756E-01	-4.2218E-01	4.5612E-01	-1.8660E-01
2.3357E-01	-8.5331E-02	1.2472E-01	-3.6774E-02
6.5550E-02	-1.117CE-02	3.0984E-02	3.1594E-03
7.0292E-03	1.2447E-02	-8.3724E-03	1.7686E-02
-1.6335E-02	1.9671E-02	-2.0066E-02	1.9872E-02
-2.1344E-02	1.9082E-02	-2.1197E-02	1.7749E-02
-2.0246E-02	1.6152E-02	-1.8901E-02	1.4467E-02
-1.7409E-02	1.2808E-02	-1.5705E-02	1.1010E-02
-1.3929E-02	9.1598E-03	-1.2361E-02	7.5069E-03
-1.1013E-02	6.0477E-03	-9.8677E-03	4.7627E-03
-8.8952E-03	3.6307E-03	-8.0612E-03	2.6410E-03
-7.3388E-03	1.7706E-03	-6.6915E-03	1.0042E-03
-6.1074E-03	3.3118E-04	-5.5607E-03	-2.6873E-04
-5.0378E-03	-7.9858E-04	-4.5317E-03	-1.2713E-03
-4.0310E-03	-1.7017E-03	-3.4682E-03	-2.1489E-03
-2.8260E-03	-2.6432E-03	-2.1300E-03	-3.2307E-03
-1.2740E-03	-4.2683E-03	3.5428E-04	-8.1883E-03



D I R E C T I V I T Y   F U N C T I O N

P (IN DEGREES) = 0.20000E 01	G = 0.10775E-01	0.18837E 00
P (IN DEGREES) = 0.40000E 01	G = 0.10591E-01	0.18792E 00
P (IN DEGREES) = 0.60000E 01	G = 0.10307E-01	0.18721E 00
P (IN DEGREES) = 0.80000E 01	G = 0.98903E-02	0.18619E 00
P (IN DEGREES) = 0.10000E 02	G = 0.93789E-02	0.18493E 00
P (IN DEGREES) = 0.12000E 02	G = 0.87509E-02	0.18339E 00
P (IN DEGREES) = 0.14000E 02	G = 0.80006E-02	0.18156E 00
P (IN DEGREES) = 0.16000E 02	G = 0.71555E-02	0.17951E 00
P (IN DEGREES) = 0.18000E 02	G = 0.62055E-02	0.17720E 00
P (IN DEGREES) = 0.20000E 02	G = 0.51766E-02	0.17472E 00
P (IN DEGREES) = 0.22000E 02	G = 0.40184E-02	0.17193E 00
P (IN DEGREES) = 0.24000E 02	G = 0.27818E-02	0.16898E 00
P (IN DEGREES) = 0.26000E 02	G = 0.14580E-02	0.16584E 00
P (IN DEGREES) = 0.28000E 02	G = 0.56949E-04	0.16255E 00
P (IN DEGREES) = 0.30000E 02	G = -0.14178E-02	0.15910E 00
P (IN DEGREES) = 0.32000E 02	G = -0.29704E-02	0.15550E 00
P (IN DEGREES) = 0.34000E 02	G = -0.46084E-02	0.15174E 00
P (IN DEGREES) = 0.36000E 02	G = -0.63234E-02	0.14784E 00
P (IN DEGREES) = 0.38000E 02	G = -0.80513E-02	0.14395E 00
P (IN DEGREES) = 0.40000E 02	G = -0.98688E-02	0.13990E 00
P (IN DEGREES) = 0.42000E 02	G = -0.11724E-01	0.13583E 00
P (IN DEGREES) = 0.44000E 02	G = -0.13636E-01	0.13168E 00
P (IN DEGREES) = 0.46000E 02	G = -0.15568E-01	0.12754E 00
P (IN DEGREES) = 0.48000E 02	G = -0.17549E-01	0.12336E 00
P (IN DEGREES) = 0.50000E 02	G = -0.19556E-01	0.11918E 00
P (IN DEGREES) = 0.52000E 02	G = -0.21609E-01	0.11497E 00
P (IN DEGREES) = 0.54000E 02	G = -0.23665E-01	0.11083E 00
P (IN DEGREES) = 0.56000E 02	G = -0.25761E-01	0.10666E 00
P (IN DEGREES) = 0.58000E 02	G = -0.27838E-01	0.10262E 00
P (IN DEGREES) = 0.60000E 02	G = -0.29954E-01	0.98552E-01
P (IN DEGREES) = 0.62000E 02	G = -0.32059E-01	0.94578E-01
P (IN DEGREES) = 0.64000E 02	G = -0.34149E-01	0.90696E-01
P (IN DEGREES) = 0.66000E 02	G = -0.36251E-01	0.86844E-01
P (IN DEGREES) = 0.68000E 02	G = -0.38324E-01	0.83103E-01
P (IN DEGREES) = 0.70000E 02	G = -0.40400E-01	0.79396E-01
P (IN DEGREES) = 0.72000E 02	G = -0.42446E-01	0.75788E-01
P (IN DEGREES) = 0.74000E 02	G = -0.44439E-01	0.72304E-01
P (IN DEGREES) = 0.76000E 02	G = -0.46416E-01	0.68859E-01
P (IN DEGREES) = 0.78000E 02	G = -0.48340E-01	0.65518E-01
P (IN DEGREES) = 0.80000E 02	G = -0.50210E-01	0.62261E-01
P (IN DEGREES) = 0.82000E 02	G = -0.52026E-01	0.59077E-01
P (IN DEGREES) = 0.84000E 02	G = -0.53782E-01	0.55953E-01
P (IN DEGREES) = 0.86000E 02	G = -0.55471E-01	0.52890E-01
P (IN DEGREES) = 0.88000E 02	G = -0.57070E-01	0.49918E-01
P (IN DEGREES) = 0.89782E 02	G = -0.58451E-01	0.47258E-01
P (IN DEGREES) = 0.92000E 02	G = -0.60060E-01	0.44027E-01
P (IN DEGREES) = 0.94000E 02	G = -0.61444E-01	0.41090E-01
P (IN DEGREES) = 0.96000E 02	G = -0.62722E-01	0.38203E-01
P (IN DEGREES) = 0.98000E 02	G = -0.63928E-01	0.35282E-01
P (IN DEGREES) = 0.10000E 03	G = -0.65021E-01	0.32400E-01

P (IN DEGREES) =	0.10200E 03	G =	-0.66039E-01	0.29461E-01
P (IN DEGRFFS) =	0.10400E 03	G =	-0.66990E-01	0.26444E-01
P (IN DFGRFFS) =	0.10600E 03	G =	-0.67839E-01	0.23422E-01
P (IN DEGRFES) =	0.10800E 03	G =	-0.68621E-01	0.20315E-01
P (IN DEGRFES) =	0.11000E 03	G =	-0.69330E-01	0.17134E-01
P (IN DEGREES) =	0.11200E 03	G =	-0.69956E-01	0.13912E-01
P (IN DFGRFFS) =	0.11400E 03	G =	-0.70558E-01	0.10529E-01
P (IN DEGRFES) =	0.11600E 03	G =	-0.71087E-01	0.70984E-02
P (IN DEGREES) =	0.11800E 03	G =	-0.71581E-01	0.35549E-02
P (IN DFGRFES) =	0.12000E 03	G =	-0.72055E-01	-0.12017E-03
P (IN DEGRFES) =	0.12200E 03	G =	-0.72480E-01	-0.38420E-02
P (IN DEGRFES) =	0.12400E 03	G =	-0.72908E-01	-0.77005E-02
P (IN DEGRFFS) =	0.12600E 03	G =	-0.73318E-01	-0.11629E-01
P (IN DFGRFES) =	0.12800E 03	G =	-0.73728E-01	-0.15641E-01
P (IN DFGRFFS) =	0.13000E 03	G =	-0.74148E-01	-0.19738E-01
P (IN DEGREES) =	0.13200E 03	G =	-0.74574E-01	-0.23884E-01
P (IN DEGRFFS) =	0.13400E 03	G =	-0.75027E-01	-0.28097E-01
P (IN DFGRFES) =	0.13600E 03	G =	-0.75496E-01	-0.32335E-01
P (IN DFGRFFS) =	0.13800E 03	G =	-0.75995E-01	-0.36600E-01
P (IN DEGREES) =	0.14000E 03	G =	-0.76507E-01	-0.40834E-01
P (IN DEGREES) =	0.14200E 03	G =	-0.77067E-01	-0.45092E-01
P (IN DEGRFES) =	0.14400E 03	G =	-0.77679E-01	-0.68826E-01
P (IN DEGRFFS) =	0.14600E 03	G =	-0.78213E-01	-0.53374E-01
P (IN DEGREES) =	0.14800E 03	G =	-0.78822E-01	-0.57406E-01
P (IN DFGRFES) =	0.15000E 03	G =	-0.79450E-01	-0.61336E-01
P (IN DEGRFES) =	0.15200E 03	G =	-0.80096E-01	-0.65168E-01
P (IN DEGRFFS) =	0.15400E 03	G =	-0.80739E-01	-0.68826E-01
P (IN DFGRFFS) =	0.15600E 03	G =	-0.81355E-01	-0.72274E-01
P (IN DEGRFES) =	0.15800E 03	G =	-0.81974E-01	-0.75556E-01
P (IN DEGREES) =	0.16000E 03	G =	-0.82562E-01	-0.78603E-01
P (IN DEGREES) =	0.16200E 03	G =	-0.83130E-01	-0.81438E-01
P (IN DEGRFFS) =	0.16400E 03	G =	-0.83677E-01	-0.84051E-01
P (IN DEGREES) =	0.16600E 03	G =	-0.84149E-01	-0.86334E-01
P (IN DEGREES) =	0.16800E 03	G =	-0.84595E-01	-0.88380E-01
P (IN DEGRFES) =	0.17000E 03	G =	-0.84989E-01	-0.90148E-01
P (IN DFGRFFS) =	0.17200E 03	G =	-0.85311E-01	-0.91591E-01
P (IN DEGRFES) =	0.17400E 03	G =	-0.85570E-01	-0.92731E-01
P (IN DEGRFES) =	0.17600E 03	G =	-0.85749E-01	-0.93531E-01
P (IN DEGRFFS) =	0.17800E 03	G =	-0.85845E-01	-0.93989E-01

R A D I A T I O N   P A T T E R N

P ( IN DEGREEES ) =	2.00000	SPL =	0.0
P ( IN DEGREEES ) =	4.00000	SPL =	-0.02158
P ( IN DEGREEES ) =	6.00000	SPL =	-0.05475
P ( IN DEGREEES ) =	8.00000	SPL =	-0.10308
P ( IN DEGREEES ) =	9.99999	SPL =	-0.16344
P ( IN DEGREEES ) =	12.00000	SPL =	-0.23717
P ( IN DEGREEES ) =	13.99999	SPL =	-0.32579
P ( IN DEGREEES ) =	15.99999	SPL =	-0.42617
P ( IN DEGREEES ) =	17.99998	SPL =	-0.53991
P ( IN DEGREEES ) =	19.99998	SPL =	-0.66416
P ( IN DEGREEES ) =	21.99998	SPL =	-0.80510
P ( IN DEGREEES ) =	23.99998	SPL =	-0.95663
P ( IN DEGREEES ) =	25.99998	SPL =	-1.12046
P ( IN DEGREEES ) =	27.99998	SPL =	-1.29513
P ( IN DEGREEES ) =	29.99998	SPL =	-1.48098
P ( IN DEGREEES ) =	31.99998	SPL =	-1.67860
P ( IN DEGREEES ) =	33.99998	SPL =	-1.88865
P ( IN DEGREEES ) =	35.99998	SPL =	-2.11106
P ( IN DEGREEES ) =	37.99998	SPL =	-2.33665
P ( IN DEGREEES ) =	39.99998	SPL =	-2.57668
P ( IN DEGREEES ) =	41.99998	SPL =	-2.82276
P ( IN DEGREEES ) =	43.99998	SPL =	-3.07809
P ( IN DEGREEES ) =	45.99998	SPL =	-3.33756
P ( IN DEGREEES ) =	47.99998	SPL =	-3.60422
P ( IN DEGREEES ) =	49.99997	SPL =	-3.87513
P ( IN DEGREEES ) =	51.99998	SPL =	-4.15205
P ( IN DEGREEES ) =	53.99997	SPL =	-4.42802
P ( IN DEGREEES ) =	55.99997	SPL =	-4.70807
P ( IN DEGREEES ) =	57.99997	SPL =	-4.98151
P ( IN DEGREEES ) =	59.99995	SPL =	-5.25761
P ( IN DEGREEES ) =	61.99995	SPL =	-5.52644
P ( IN DEGREEES ) =	63.99994	SPL =	-5.78706
P ( IN DEGREEES ) =	65.99992	SPL =	-6.04222
P ( IN DEGREEES ) =	67.99997	SPL =	-6.28481
P ( IN DEGREEES ) =	69.99995	SPL =	-6.51867
P ( IN DEGREEES ) =	71.99994	SPL =	-6.73778
P ( IN DEGREEES ) =	73.99994	SPL =	-6.93963
P ( IN DEGREEES ) =	75.99992	SPL =	-7.12864
P ( IN DEGREEES ) =	77.99997	SPL =	-7.29994
P ( IN DEGREEES ) =	79.99995	SPL =	-7.45450
P ( IN DEGREEES ) =	81.99994	SPL =	-7.59291
P ( IN DEGREEES ) =	83.99992	SPL =	-7.71632
P ( IN DEGREEES ) =	85.99997	SPL =	-7.82502
P ( IN DEGREEES ) =	87.99995	SPL =	-7.91887
P ( IN DEGREEES ) =	89.78242	SPL =	-7.99430
P ( IN DEGREEES ) =	91.99994	SPL =	-8.07513
P ( IN DEGREEES ) =	93.99992	SPL =	-8.13969
P ( IN DEGREEES ) =	95.99997	SPL =	-8.19593
P ( IN DEGREEES ) =	97.99995	SPL =	-8.24600
P ( IN DEGREEES ) =	99.99994	SPL =	-8.29031

P (IN DEGREES) =	101.99992	SPL =	-8.33032
P (IN DEGREES) =	103.99992	SPL =	-8.36553
P (IN DEGREES) =	105.99995	SPL =	-8.39595
P (IN DEGREES) =	107.99995	SPL =	-8.42063
P (IN DEGREES) =	109.99994	SPL =	-8.43876
P (IN DEGREES) =	111.99992	SPL =	-8.44967
P (IN DEGREES) =	113.99991	SPL =	-8.44802
P (IN DEGREES) =	115.99995	SPL =	-8.43578
P (IN DEGREES) =	117.99994	SPL =	-8.40801
P (IN DEGREES) =	119.99992	SPL =	-8.36134
P (IN DEGREES) =	121.99992	SPL =	-8.29810
P (IN DEGREES) =	123.99991	SPL =	-8.21097
P (IN DEGREES) =	125.99995	SPL =	-8.10250
P (IN DEGREES) =	127.99994	SPL =	-7.97084
P (IN DEGREES) =	129.99992	SPL =	-7.81528
P (IN DEGREES) =	131.99991	SPL =	-7.63880
P (IN DEGREES) =	133.99995	SPL =	-7.44030
P (IN DEGREES) =	135.99994	SPL =	-7.22463
P (IN DEGREES) =	137.99994	SPL =	-6.99298
P (IN DEGREES) =	139.99992	SPL =	-6.75201
P (IN DEGREES) =	141.99991	SPL =	-6.49860
P (IN DEGREES) =	153.99994	SPL =	-5.00090
P (IN DEGREES) =	145.99994	SPL =	-5.98865
P (IN DEGREES) =	147.99992	SPL =	-5.73352
P (IN DEGREES) =	149.99991	SPL =	-5.48242
P (IN DEGREES) =	151.99991	SPL =	-5.23611
P (IN DEGREES) =	153.99994	SPL =	-5.00090
P (IN DEGREES) =	155.99994	SPL =	-4.78029
P (IN DEGREES) =	157.99992	SPL =	-4.57048
P (IN DEGREES) =	159.99991	SPL =	-4.37692
P (IN DEGREES) =	161.99989	SPL =	-4.19759
P (IN DEGREES) =	163.99994	SPL =	-4.03279
P (IN DEGREES) =	165.99992	SPL =	-3.89058
P (IN DEGREES) =	167.99991	SPL =	-3.76320
P (IN DEGREES) =	169.99991	SPL =	-3.65359
P (IN DEGREES) =	171.99994	SPL =	-3.56479
P (IN DEGREES) =	173.99994	SPL =	-3.49486
P (IN DEGREES) =	175.99992	SPL =	-3.44610
P (IN DEGREES) =	177.99991	SPL =	-3.41862